The use of Cone Beam Computed Tomography for implant treatment planning at UBC

by

AMANDEEP HANS

B.Sc., The University of British Columbia, 2008

DMD, The University of British Columbia, 2013

A THESIS SUBMITTED IN PARTIAL FULFILLMENT OF

THE REQUIREMENTS FOR THE DEGREE OF

MASTER OF SCIENCE

in

THE FACULTY OF GRADUATE AND POSTDOCTORAL STUDIES

(Craniofacial Science)

THE UNIVERSITY OF BRITISH COLUMBIA

(Vancouver)

August 2020

The following individuals certify that they have read, and recommend to the Faculty of Graduate and Postdoctoral Studies for acceptance, the dissertation entitled:

The use of Cone Beam Computed Tomography for implant treatment planning at UBC

submitted by Amandeep Hans in partial fulfillment of the requirements for

the degree of Master of Science

in Craniofacial Science

Examining Committee:

Dr. David Macdonald – Faculty of Dentistry
Supervisor

Dr. Flavia Lakschevitz – Faculty of Dentistry
Supervisory Committee Member

Dr. Babak Chehroudi – Faculty of Dentistry
Supervisory Committee Member

Dr. Siddharth Vora – Faculty of Dentistry
University Examiner

Abstract

Purpose: Cone beam computed tomography (CBCT) has become the standard of care for many applications in the specialty of periodontics. CBCT is now taken for almost all implant related cases and there is also a clear shift towards higher resolution images. However, the increased radiation dosage from a higher resolution images must be accompanied by valid clinical justification.

Aims: The first aim was to conduct an audit of all CBCT prescriptions at the UBC Faculty of Dentistry with a focus on implant related prescriptions. Concurrently, all implant related prescriptions were evaluated for compliance with the current guidelines. The second aim was to evaluate whether altering the mA and kVp values will result in measurement differences on CBCT images.

Materials and Methods: Ethics approval was granted for the retrospective portion of this study (Certificates H18-01536 and H19-02001). All CBCT prescriptions were audited from Jan. 1, 2015 to Aug. 31, 2018. However, the prescriptions originating from the Graduate Periodontics and Prosthodontics programs were examined more thoroughly. A major finding from the audit was a shift towards higher resolution images for the small FOV. An *in vitro* experiment was conducted to determine whether changing the imaging parameters and scatter would affect the measured distance between two adjacent implants placed in a model.

Results: Almost all the CBCT scans prescribed in the Periodontics and Prosthodontics departments were prescribed for the purposes of implant treatment planning. In Graduate Periodontics and Prosthodontics, 95% and 94% of the prescriptions, respectively, were compliant with the guidelines published by the AAOMR and the AAP. Manipulation of the imaging parameters did affect the measured distance between the two implants when specific mA and kVp values were compared. The scatter and metal artifacts from the addition of a third implant did not have any effect on the measured distance.

Conclusion: CBCT was used judiciously for implant treatment planning in both the Graduate Periodontics and Prosthodontics department. Manipulation of CBCT parameters had a statistically significant effect on the measured distance between two adjacent implants but the potential scatter and metal artifacts from the addition of third implant did not.

Lay Summary

Cone Beam Computed Tomography (CBCT) has been used in dentistry for over 20 years. Due to its many advantages, it has become the standard of care for dental implants. However, the radiation dosage from CBCT is much higher than the usual dental X-ray techniques. Therefore, it should be used judiciously, and the published guidelines should always be followed when prescribing CBCTs. We reviewed the records of all patients for whom a CBCT was taken between 1st January 2015 and 31st August 2018. We focused mainly on those made for the purposes of dental implants. Two major findings were revealed in the audit. First, that the CBCTs were largely in compliance with the guidelines from the American Academy of Oral and Maxillofacial Radiology and the American Academy of Periodontology. Second, that there was a distinct shift towards better detailed scans, which are accompanied by higher radiation dosage. We wanted to further evaluate whether changing the exposure factors and image quality will affect the measured distance between two adjacent implants. The results revealed that certain changes in the exposure will indeed affect the measured distance.

Preface

I conducted this retrospective and in-vitro study under the valuable guidance and support of my supervisor, Dr. David MacDonald, and my research committee members, Dr. Flavia Lakschevitz and Dr. Babak Chehroudi.

I was responsible for collecting the data for the CBCT cases in the Faculty of Dentistry for Part 1 of this study.

For the *in vitro* portion of this study, I planned the implant position and fabricated the guide under the guidance of Dr. Lakschevitz. I took all the necessary CBCT scans and performed the measurements. Dr. Lakschevitz helped me immensely with the statistical analysis and Dr. Chehroudi provided valuable feedback.

Ethics approval certificates were granted for all parts of this study from UBC Clinic Research Ethics Board (Certificate number: H18-01536 and H19-02001)

Table of Contents

Abstract .... **ii**

Lay Summary .... **iv**

Preface .... **v**

Table of Contents .... **vi**

List of Tables .... **ix**

List of Figures .... **xi**

List of Abbreviations .... **xiii**

Acknowledgements .... **xiv**

Dedication .... **xv**

Chapter 1: Introduction **1**

1.1 Introduction to Radiation Physics 1

1.2 Two-dimensional imaging in Periodontics 2

1.2.1 Intraoral Radiographs – Periapical radiographs and Bitewings 2

1.2.2 Extraoral Imaging – Panoramic Radiographs 3

1.2.3 Disadvantages of two-dimensional imaging 3

1.3 Cone-beam Computed Tomography 4

1.3.1 Image acquisition within a CBCT system 4

1.3.2 Advantages of CBCT 5

1.3.3 Disadvantages of CBCT 6

1.3.4 Indications for CBCT in Periodontics 7

1.4 Research Aims 11

Chapter 2: Materials and Methods 13

2.1.1 Audit of CBCT referrals 13

2.1.2 Implant related audit of Graduate Periodontics and Prosthodontics programs......... 15

2.2 Variation of CBCT Parameters 15

2.2.1 Virtual planning 16

2.2.2 Placement of Implants... 21

2.2.3 CBCT image acquisition.. 24

2.2.4 Measurements and Data Collection 29

2.3 Statistical Analysis.. 33

Chapter 3: Results...35

3.1 CBCT Audit from Jan. 2015 to Aug. 2018.. 35

3.2 Compliance with published recommendations 43

3.3 Manipulation of CBCT parameters... 45

3.3.1 Measurements between implants 45

3.3.2 Relationship between mA and measurements for small and medium FOVs (2 implants) 46

3.3.3 Relationship between kVp and measurements for small and medium FOVs (2 implants) 47

3.3.4 Comparing measurements between small and medium FOV scans with 2 implants 49

3.3.5 Addition of third implant 50

Chapter 4: Discussion 52

4.1 CBCT Audit.. 52

4.2 Observance of guidelines.. 57

4.3 CBCT imaging parameters ... 59

4.4 Limitations ... 63

4.5 Future Directions ... 65

Chapter 5: Conclusions ... 67

5.1 Part 1 ... 67

5.2 Part 2 ... 67

5.3 Part 3 ... 67

Bibliography ... 69

Appendices ... 77

Appendix A ... 77

Appendix B ... 80

Appendix C ... 86

Appendix D ... 92

List of Tables

Table 1: AAMOR recommendations regarding the use of CBCT for implants 9

Table 2: AAP conclusions relating to the use of CBCT for implant treatment planning 10

Table 3: Parameters used for small Field of View scans – varying mA...................................... 26

Table 4: Parameters used for small Field of View scans – varying kVp 26

Table 5: Parameters used for the medium Field of View scans - varying mA 27

Table 6: Parameters used for medium Field of View scans - varying kVp 27

Table 7: Number and percentages of CBCTs taken by all disciplines at UBC 36

Table 8: CBCT prescriptions in the Graduate Periodontics program 37

Table 9: CBCT prescriptions in the Graduate Prosthodontics program 38

Table 10: Number and percentages of males and females in the Graduate Periodontics program 38

Table 11: Number and percentages of males and females in the Graduate Prosthodontics program 39

Table 12: Fields of view in the Graduate Periodontics program 40

Table 13: Fields of view in the Graduate Prosthodontics program 41

Table 14: Location of scans in the Graduate Periodontics program 42

Table 15: Location of scans in the Graduate Prosthodontics program 42

Table 16: Statistically significant differences for small field of view scans with 2 implants comparing kVp 48

Table 17: Statistically significant differences for medium field of view scans with 2 implants comparing kVp 49

Table 18: Statistically significant differences between small and medium fields of view at varying mA values 50

Table 19: P-values for various comparisons after addition of a third implant............................. 51

List of Figures

Figure 1: Fields of view available in the Carestream 9300 at UBC Faculty of Dentistry 14

Figure 2: Carestream 9300 cone-beam computed tomography machine at UBC 14

Figure 3: Occlusal view of the model mandible for implant placement...................................... 17

Figure 4: Side view of the model mandible used for implant placement 17

Figure 5: Stereolithography of model mandible generated by the intraoral 3-D scanner............. 18

Figure 6: Model mandible placed in the Carestream 9300 machine for CBCT acquisition......... 19

Figure 7: DICOM file of model mandible imported from Carestream 9300................................ 20

Figure 8: Virtual planning in Blue Sky Plan 4 implant planning software................................... 21

Figure 9: Virtual planning of surgical guide in the Blue Sky Plan 4 software 21

Figure 10: Surgical guide after fabrication and processing 22

Figure 11: Surgical guide fitted to the model 23

Figure 12: Straumann 4.1x10mm bone level implant placed using the guide.............................. 23

Figure 13: Implant position after removal of guide 24

Figure 14: Model glued to foam insert that fits precisely into a platform within Carestream 9300 25

Figure 15: Image acquisition after placement of 3rd implant on the right side 29

Figure 16: Parallelism between the reference line and measurements 31

Figure 17: Axial view illustrating the overlap between the reference line and measurement 33

Figure 18: Number of CBCTs taken by each discipline 36

Figure 19: Implant related prescriptions in Graduate Periodontics and Prosthodontics programs38

Figure 20: Comparison of males and females for CBCT in the Periodontics and Prosthodontics programs 39

Figure 21: Age distribution of CBCT Prescriptions in the Periodontics and Prosthodontics programs 40

Figure 22: Fields of view comparison between the Graduate Periodontics and Prosthodontics programs 41

Figure 23: Comparison of sites between the Graduate Periodontics and Prosthodontics Programs 42

Figure 24: Conventional image prior to CBCT in the Graduate Periodontics program 43

Figure 25: Type of 2-D image prior to 3-D image in the Graduate Periodontics program 44

Figure 26: Conventional image prior to CBCT in the Graduate Prosthodontics program 44

Figure 27: Type of 2-D image prior to 3-D image in the Graduate Prosthodontics program....... 45

Figure 28: Mean difference in implant distance at various mA values compared to 2mA for small FOV.. 46

Figure 29: Mean difference in implant distance at various mA values compared to 2mA for small FOV.. 47

List of Abbreviations

2D	Two dimensional
3D	Three dimensional
AAOMR	American Academy of Oral and Maxillofacial Radiology
AAP	American Academy of Periodontology
ALARA	As Low as Reasonably Achievable
CBCT	Cone Beam Computed Tomography
CT	Computed Tomography
DAP	Dose Area Product
DF	Degrees of Freedom
EHR	Electronic Health Record
EPR	Electronic Patient Record
FOV	Field of View
kVp	Peak voltage
mA	Milliamperage
mm	Millimeter
MS	Mean squares
ns	Nonsignificant
SS	Sum of squares

Acknowledgements

I am deeply grateful for all the direction, encouragement, and support provided to me by my supervisor, Dr. David MacDonald. Although I came across many obstacles while conducting this research, I was able to navigate around them through my supervisor's guidance.

I would like to sincerely thank Dr. Flavia Lakschevitz for being an immense help in conducting the second part of this project and statistics. Dr. Lakschevitz always took the time out of her busy schedule and made herself available whenever I asked for help.

I would like to sincerely thank Dr. Babak Chehroudi for his insightful feedback and having the foresight to see some of the early pitfalls I would have otherwise fallen into.

I would also like to express my gratitude towards my co-residents. Their continuous support is what helped me through all the long days spent conducting my research.

Finally, innumerous thanks are owed to my wife and parents, who have been my pillars of strength.

Dedication

This is dedicated to my wife and parents.

Chapter 1: Introduction

Use of radiology in Periodontics

Radiographic imaging is an essential part of the practice of dentistry. Used in conjunction with clinical examination, imaging forms a vital part of the work-up. It helps the clinician in making an accurate diagnosis for the patient and subsequently developing an appropriate treatment plan (Chakrapani et. al 2013). Like other disciplines in dentistry, radiology is a critical element in the speciality of periodontics. Although two-dimensional imaging modalities such as periapical radiographs, bitewing radiographs and panoramic images are used more commonly in periodontology, three-dimensional imaging has quickly gained popularity due to it's several advantages. Regardless of the type of imaging to be utilized, the clinician should be guided by the ALARA principle and select the least invasive technique with the lowest radiation exposure but that, concurrently, will also yield the necessary information (Chakrapani et. al 2013).

1.1 Introduction to Radiation Physics

X-rays fall within the high-energy range of the electromagnetic spectrum and are capable of ionizing matter (White and Pharoah 8e, Page 31). Within an X-ray machine, these ionizing rays are produced by the X-ray tube (White and Pharoah 8e, Page 34). The X-ray tube consists of a cathode and an anode, which are oppositely charged and separated by a vacuum (Pauwels et. al 2015). The cathode contains a filament, which is the electron source within the X-ray tube (White and Pharoah 8e, Page 35). When this filament is heated, it results in the release of electrons directly proportional to the temperature of the filament itself (White and Pharoah 8e, Page 36). These electrons then strike a small rectangular area known as the focal spot on the anode, resulting in the production of X-ray photons (White and Pharoah 8e, Page 37). The X-rays then pass through the patient's tissues and strike the detector (White and Pharoah 8e, Page 34). The X-ray detectors convert these X-rays into an electrical signal, resulting in the formation of a radiographic image (Pauwels et. al 2015). The number of electrons produced by the filament within the cathode are directly affected the tube current, measured in milliamperes (mA) (White and Pharoah 8e, Page 40). The peak energy of these electrons is regulated by the tube voltage, which is measured in kilovolts (kV) (White and Pharoah 8e, Page 40). In addition to the tube current and tube voltage, the X-ray beam is also affected by shape (filtration and collimation) and exposure time (White and Pharoah 8e, Page 48). Filtration refers to removal of certain X-rays that will not pass through the patient (Pauwels et. al 2015).

1.2 Two-dimensional imaging in Periodontics

1.2.1 Intraoral Radiographs – Periapical radiographs and Bitewings

Intraoral radiographs consist of two-dimensional images, typically representing a small area of the oral cavity (Lindhe 6e, Page 593). Periapical radiographs are used to visualize the apex and the bone morphology around teeth (Chakrapani et. al 2013). Improper angulation of the periapical radiographs can distort crestal alveolar bone levels and therefore paralleling technique should be used whenever possible (Chakrapani et. al 2013, Lindhe 6e, Page 594). Bitewing radiographs, both in horizontal and vertical orientation, are usually more accurate and therefore the preferred method for assessing bone levels in periodontology (Lindhe 64, Page 594).

The major advantage of intraoral radiographs is their superior image quality including contrast, clarity and detail (Kim et. al 2017). Furthermore, this imaging type is readily available in most dental offices, tolerated well by patients and inexpensive compared to other modalities.

1.2.2 Extraoral Imaging – Panoramic Radiographs

In addition to intraoral radiographs, panoramic radiographs are also commonly used by many general dentists and specialists. Panoramic radiographs can provide an overall view of the jaws including the periodontium (Chakrapani et. al 2013). Consequently, many anatomic structures and features can be visualized in a single film. The radiation dosage of a single panoramic radiograph is also usually lower than multiple intraoral radiographs (Vijay et. al 2013). Like intraoral imaging, panoramic radiographs are readily available and can be obtained at a relatively low cost (Tyndall et. al 2000). However, when fine detail is required to be visualized, intraoral radiographs may be required to supplement a panoramic image.

1.2.3 Disadvantages of two-dimensional imaging

Disadvantages of intraoral films include difficulty in reproducibility and image distortion intrinsic to the modality itself (Tyndall et. al 2000). Occasionally, the patient may present with anatomic limitations, such as presence of tori or a shallow palatal vault, that make paralleling technique impossible (Patel et. al 2015). Inability to utilize the paralleling technique will increase the amount of geometric distortion in the image. The major disadvantage of all two-dimensional imaging strategies, however, is that they are limited in providing information about structures or changes that are occurring in three-dimensions (Tyndall et. al 2000, Kim et. al 2017). For example, for intrabony and furcation defects only the depth and mesiodistal dimension can be determined in conventional two-dimensional imaging (Kim et. al 2017). The bucco-lingual width of such defects is impossible to resolve from these radiographs. Furthermore, if there is periodontal destruction of hard tissue that is confined to the buccal or lingual aspects of teeth, it cannot be appreciated using conventional radiography (Vijay et. al 2013). Moreover, superimposition of anatomic structures on two-dimensional images can sometimes obscure information that may be of interest to the clinician (Kim et. al 2017). For instance, highly mineralized anatomic structures such as the external oblique ridge and zygomatic arch can often obscure adjacent defects (Lindhe 6e, Page 594). Additionally, a sufficient amount of demineralization of hard tissue must have occurred before it can be visualized on two-dimensional imagining. Consequently, there is a potential to miss lesions such as narrow vertical defects or horizontal defects where buccal and/or lingual cortices are still present (Lindhe 6e, Page 594).

For panoramic radiographs, the main disadvantage is image distortion (Kim et. al 2017, Lindhe 6e, Page 596). Lower resolution, overlapping structures, ghost images, anatomic structure presenting as blurry, magnification, and varying foreshortening and elongation are also all shortcomings specific to panoramic films (Kim et. al 2017, Lindhe 6e, Page 596). Although panoramic radiographs can provide a rough estimate of the size of anatomic structures, lesions etc., it is severely inadequate when accurate dimensions are essential (Lindhe 6e, Page 597)

1.3 Cone-beam Computed Tomography

Although Computed Tomography was first shown to be an advantageous radiographic technique for preoperative assessment for implant planning in the late 1980s (Schwarz et. al 1987), it wasn’t until 2000 that Cone Beam Computed Tomography was advocated by Tyndall et. al in a position paper published by the American Academy of Oral and Maxillofacial Radiology. CBCT scanners themselves were introduced to dentistry in the late 1990s (Pauwels et. al 2015).

1.3.1 Image acquisition within a CBCT system

CBCT projects a cone-shaped beam from an X-ray source onto a detector (MacDonald, 2011 page 60). The detector and the X-ray source rotate simultaneously and can rotate up to 360 degrees in a single rotation (MacDonald, 2011 page 59). This rotation can last between 10 and 40 seconds (Pauwels et. al 2015). Several hundred two-dimensional image are acquired by the detector during this rotation (Pauwels et. al 2015). The series of projections acquired can then be reconstructed into a three-dimensional image in the reconstruction software (Pauwels et. al 2015). As opposed to pixels, which make up two-dimensional images, CBCT images are composed of voxels (Pauwels et. al 2015). The size of voxels is directly related to spatial resolution of a volume, with machines capable of generating smaller voxels providing greater resolution (Pauwels et. al 2015). The size of the voxels is much smaller in CBCT when compared to a multi-slice CT (Macdonald, 2020 page 93). In contrast to a multi slice CT, CBCT is smaller in size, cheaper, delivers a lower radiation dosage and provides higher spatial resolution (Watanabe et. al 2019).

1.3.2 Advantages of CBCT

There are distinct advantages of CBCT when compared to two-dimensional imaging. The amount of diagnostic information and increase in accuracy that can be obtained from CBCT is simply not possible with any conventional imaging technique (Mandelaris et. al 2017). The absence of distortion and overlapping in CBCT allows for a greater amount of information to be collected (Misch et. al 2006). CBCT images are also an effective communication tool when it comes to corresponding with patients and colleagues from other specialties (Mandelaris et. al 2017).

The overall effect of these advantages is invaluable in evaluating, diagnosing, and planning complex cases especially when treatment involves surgical management (Mandelaris et. al 2017).

1.3.3 Disadvantages of CBCT

The spatial resolution of CBCT is still far inferior to that of intraoral imaging (MacDonald 2020, page 94). Therefore, it is still unable to display changes in appearance of the bone such as "ground-glass" and "peau d'orange" that are associated with certain pathological conditions (MacDonald 2020, page 94). Furthermore, CBCT images can suffer from beam hardening and metal artifacts when metal restorations are present intraorally (Kim et. al 2017, MacDonald 2020, page 103). Both beam hardening and metal artifacts degrade image quality.

It is also well established the total radiation dosage from a CBCT is much higher than that received by the patient for typical panoramic radiograph or a full mouth series (American Dental Association Council on Scientific Affairs, 2012, Bornstein et. al 2014, MacDonald 2020, page 101). The evidence for long-term effects of cumulative radiation dose from CBCT is lacking and risks are currently unknown (Mandelaris et. 2017). It is important to note that when principles of limiting radiation exposure are followed carefully, the risk from increased radiation dose from CBCT is estimated to be low (Mandelaris et. al 2017). However, younger sect of the population may be especially vulnerable to the effects of ionizing radiation. A greater incidence of cancer has been reported in those exposed to CT scans at a young age. (MacDonald 2020, page 103). Acquisition parameters such as milliamperage, kilovoltage, voxel size and field-of-view have a substantial impact on both image quality and radiation dose received by the patient (Katsumata et. al 2009, Bornstein et. al 2014). Therefore, CBCT imaging should be prescribed judiciously and imaging parameters carefully selected, especially when exposing those who are most susceptible to the risks of increased radiation such as children.

1.3.4 Indications for CBCT in Periodontics

Although conventional two-dimensional imaging is adequate for many clinical situations, CBCT may be advantageous for certain scenarios. Dental implant therapy remains the major indication for the utilization of cross-sectional imaging. However, dental implants have been placed with a high degree of predictability and success with the utilization of conventional two-dimensional imaging modalities for over 30 years (Bornstein et. al 2014). Due to the increased radiation and monetary cost for the patient, the use of cross-sectional imaging must demonstrate distinct benefits over two-dimensional imaging for all purposes including implant therapy (Bornstein et. al 2014). CBCT should only be utilized when conventional imaging has proven to be insufficient in diagnosing and treatment planning. Clinical complexity, local anatomic considerations, possible risk of complications and esthetic importance should be considered when selecting the type of imaging (Bornstein et. al 2014). Imaging should be able to provide information regarding the morphologic characteristics and orientation of the residual alveolar ridge (Bornstein et. al 2014). Furthermore, the anatomic and pathologic limits within which an implant can or cannot be placed should be established through imaging prior to commencing any treatment (Bornstein et. al 2014). CBCT satisfies majority of these requirements. CBCT can identify many anatomic structures including, but not limited to, the anterior loop and mandibular incisive canal, mental foramen, lingual canal, submandibular gland fossa, lingual concavity and maxillary incisive canal that may not readily be identifiable on two-dimensional imaging (Bornstein et. al 2014). Detection of these anatomic structure is critical for implant treatment planning. In patients with permanent inferior alveolar nerve neuropathy related to dental implant placement, only 10% of the cases were associated with the preoperative use of CBCT (Renton et. al 2012). The compartive figures for intraoral imaging and panoramic radiography were 30% and 50%, respectively (Renton et. al 2012). CBCT can also be beneficial in identification of incidental findings, such as periapical pathology, root fractures etc., that can alter the treatment plan (Mandeleris et. al 2017). Furthermore, CBCT can simplify the surgical procedure by allowing the clinician to select suitable number, size and position of implants beforehand (Bornstein et. al 2014).

Due to use of CBCT becoming widespread, the American Academy of Oral and Maxillofacial Radiology has published guidelines pertaining to its responsible use in dental implant therapy (Tyndall et. al 2012).

Initial Examination	
Recommendation 1	Panoramic radiography should be used as the imaging modality of choice in the initial evaluation of the dental implant patient.
Recommendation 2	Use intraoral periapical radiography to supplement the preliminary information from panoramic radiography.
Recommendation 3	Do not use cross-sectional imaging, including CBCT, as an initial diagnostic imaging examination.
Preoperative site-specific imaging	
Recommendation 4	The radiographic examination of any potential implant site should include cross-sectional imaging orthogonal to the site of interest.
Recommendation 5	CBCT should be considered as the imaging modality of choice for preoperative cross-sectional imaging of potential implant sites.
Recommendation 6	CBCT should be considered when clinical conditions indicate a need for augmentation procedures or site development before placement of dental implants: (1) sinus augmentation, (2) block or particulate bone grafting, (3) ramus or symphysis grafting, (4) assessment of impacted teeth in the field of interest, and (5) evaluation of prior traumatic injury.
Postoperative site-specific imaging	
Recommendation 7	CBCT imaging should be considered if bone reconstruction and augmentation procedures (e.g., ridge preservation or bone grafting) have been performed to treat bone volume deficiencies before implant placement.
Recommendation 8	In the absence of clinical signs or symptoms, use intraoral periapical radiography for the postoperative assessment of implants. Panoramic radiographs may be indicated for more extensive implant therapy cases.
Recommendation 9	Use cross-sectional imaging (particularly CBCT) immediately postoperatively only if the patient presents with implant mobility or altered sensation, especially if the fixture is in the posterior mandible.
Recommendation 10	Do not use CBCT imaging for periodic review of clinically asymptomatic implants.
Recommendation 11	Cross-sectional imaging, optimally CBCT, should be considered if implant retrieval is anticipated.

Table 1: AAMOR recommendations regarding the use of CBCT for implants

In addition to the guidelines listed above, the American Academy of Periodontology has also published a best evidence consensus statement on the applications of CBCT (Mandelaris et. al 2017).

Recommendation 1	Evaluation of root morphology and associated pathology for extractions and reconstruction
Recommendation 2	Location of relevant anatomic structures and their relation to implant placement
Recommendation 3	Sinus grafting preimplant evaluation
Recommendation 4	Evaluation of autogenous bone donor sites
Recommendation 5	Fabrication of static surgical guides and dynamic navigation of implant placement
Recommendation 6	Post-bone augmentation implant planning
Recommendation 7	Complications with previously placed implants
Recommendation 8	Team communication with implant restorative colleagues

Table 2: AAP conclusions relating to the use of CBCT for implant treatment planning

In addition to dental implant therapy, CBCT has the potential to be invaluable in the diagnosis and management of inflammatory periodontal disease, especially for teeth with intrabony defects or furcation involvement (Kim et. al 2017). The sensitivity of detection and classification of bony defects has been shown to be superior when using CBCT as compared to intraoral imaging (Misch et. al 2006). In an in-vitro study, Vandenberghe and colleagues were able to detect craters and furcation involvement 71% of the time with CBCT and only 56% of time with digital intraoral imaging (Vandenberghe et. al 2007). Some authors have also reported a more accurate assessment of crestal bone levels using cross-sectional imaging when compared to conventional two-dimensional radiography (Choi et. al 2018). An accurate diagnosis of such defects can aid in assigning a correct prognosis, formulating a justified treatment plan, avoiding unnecessary treatment, shorten treatment time and avert unexpected treatment costs (Kim et. al 2017). Although many studies have demonstrated that CBCT can be useful in assessment and treatment planning for intrabony and furcation defects, the overall body of evidence is still limited to justify its routine use in diagnosis and management of moderate-severe periodontal disease (Kim et. al 2017, Mandeleris et. al 2017).

Finally, it is important to note that the fundamental rules of radiology apply to all imaging modalities. Images should be of adequate diagnostic quality and should not extend beyond the area of interest to limit radiation exposure to the patient (Tyndall et. al 2012, Kim et. al 2017). Furthermore, adequate training in the use of CBCT equipment should be obtained and maintained by the person prescribing and/or acquiring images (Tyndall et. al 2012, Brown et. al 2014). Regardless of the type of imagine modality utilized, it cannot be emphasized enough that the entire volume needs to be reviewed by the prescribing clinician (MacDonald 2020, page 93). This is essential both for clinical and medicolegal purposes.

1.4 Research Aims

This study has the following aims:

1. Conduct an audit of all CBCT prescriptions between Jan. 1, 2015 and Aug. 31, 2018 at the Faculty of Dentistry at the University of British Columbia.
2. Check if all the implant related CBCT prescriptions are in compliance with the AAOMR and AAP guidelines.

3. Assess whether changing imaging parameters, specifically mA and kVp, will alter the measured distance in the Carestream 9300 software between two adjacent implants.
    a. Our hypotheses are as follow:
        i. Null hypothesis: There is no difference in measurements between two implants when imaging parameters are altered in the small and medium FOVs
        ii. Research hypothesis: There is a difference in measurements between two implants when imaging parameters are altered in the small and medium FOVs

Chapter 2: Materials and Methods

2.1.1 Audit of CBCT referrals

This component of the study was retrospective in nature and consisted of an audit of CBCT prescriptions. The objective of this portion of the study was to determine the pattern of prescriptions by all graduate programs at UBC with a focus on the implant related referrals. This was a continuation of an earlier study conducted by Dr. Meeta Bhatt.

A system of online referrals for CBCT has been in place at the University of British Columbia Faculty of Dentistry since 2012. These referrals are stored in a database. For the purposes of this study this database was reviewed along with patient electronic health records (EHR). All referrals made within the Faculty of Dentistry between the period of 1st January 2015 and 31st August 2018 were audited. In addition, all prescriptions made by the Graduate Periodontics and Prosthodontics programs within the same time period were assessed for quality assurance and compliance purposes. Ethics approval certificates H18-01536 and H19-02001 were granted for this portion of the study.

Graduate students at UBC are required to complete both didactic and practical training prior to being granted privileges for prescribing and taking CBCTs. This training includes knowledge in technology, diagnosis and technique, as well as a competency assessment conducted by an appropriate faculty member. Furthermore, all CBCT prescriptions are accompanied by an approval by a credentialed instructor. The department of origin, field-of-view, spatial resolution (high or low), region of interest and a short statement about the clinical indication or exact investigative motive for the CBCT prescription are included in the referral. A sample referral form can be found in Appendix A at the end. The FOVs are limited to what is allowed in the

Carestream 9300 (Carestream Dental LLC, Atlanta, USA) namely 5x5cm, 10x5cm, 8x8cm and 10x10cm as noted in the following image.

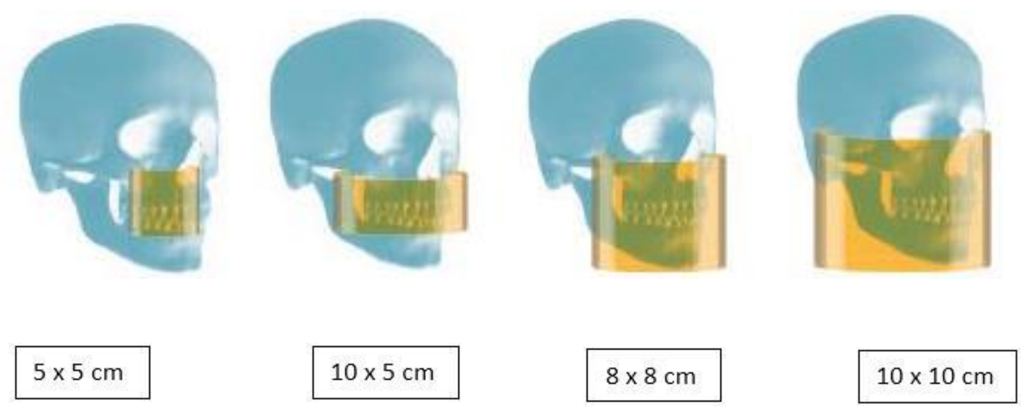

Images: https://www.carestreamdental.com/en-emea/csd-products/extraoral-imaging/cs-9600/

Figure 1: Fields of view available in the Carestream 9300 at UBC Faculty of Dentistry

The 5x5cm FOV is available in both low and high spatial resolution in the Carestream machine at UBC.

Figure 2: Carestream 9300 cone-beam computed tomography machine at UBC

2.1.2 Implant related audit of Graduate Periodontics and Prosthodontics programs

The second part of the audit consisted of a review of the CBCTs prescribed by the Graduate Periodontics and Prosthodontics programs in the period between 1st of January 2015 and 31st August 2018. The aim of this portion of the study was to review the compliance of the prescriptive pattern of the Periodontics and Prosthodontics programs with the guidelines set by the American-Academy-of-Oral-and-Maxillofacial-Radiology (AAOMR) and the American-Academy-of-Periodontics (AAP) mentioned earlier. In addition, special consideration was given to CBCT radiographs obtained for the purpose of implant treatment planning and to those patients who had multiple CBCTs taken between 1st January 2015 and 31st August 2018. The rationale behind this was to review that patients were not receiving unnecessary radiation. In other words, we attempted to answer whether CBCT was used judiciously to supplement two-dimensional imaging for implant treatment planning and that the multiple exposures were justified.

All CBCT images prescribed for the purpose of implant or implant related treatment planning by the Graduate Periodontics programs within the stated time interval were identified. The EHR for each prescription was then reviewed specifically for the presence or absence of conventional two-dimensional image i.e. peri-apical, bitewing or panoramic image prior to a CBCT referral. Furthermore, patients who were subjected to multiple CBCT scans within the stated time interval were identified and all CBCT referrals for those patients were further investigated for the presence of a justifiable clinical indication for the multiple prescriptions.

2.2 Variation of CBCT Parameters

Once the audit as outlined in Part 1 was completed, it was noted that there was a trend towards using higher resolution imaging in the Graduate Periodontics program. Presumably, the shift towards higher resolution images is due to a desire for better-quality images. Higher resolution images allow the clinician to decipher fine details, which were deemed necessary for proper diagnosis and treatment planning (Kerfeld et. al 2018). Theoretically, the ability to resolve finer details should result in increased accuracy in several measurements that are often required in implant treatment planning such as distance from vital structures, adjacent teeth etc. Spatial resolution is indirectly affected by imaging parameters such as the tube current (mA), tube potential (kVp), and exposure time, which in turn affect the radiation dose to the patient (Pauwels et. al 2015).

Therefore, the objective of part 2 of this study was to evaluate whether altering the mA and kVp values will result in changes in the measured distance between two implants on Carestream 9300 CBCT image viewer. This portion of the study was an *in vitro* design.

2.2.1 Virtual planning

A polyurethane model mandible that is commonly used in simulation implant training was used as a medium for implant placement. This model is designed to simulate bone density which can be classified as D2 i.e. dense cortical bone surrounding dense trabecular bone. This reflects what would be commonly encountered in the posterior mandible. Several studies have validated the use of polyurethane material as suitable medium for implant placement. This material closely mimics the compressive strength and modulus of elasticity of bone including that of the mandible (Neto et. al 2011, Horn et. al 2014). The model consists of a dense outer material surrounding a less dense inner core. This is also reflected radiographically in the CBCT of the model (Figure 7). A clear “cortical” outline surrounding “trabecular” bone is visible in the radiograph of this model. Although the model is not as radiographically dense as a real human mandible, it approximates it closely. However, what the model does not capture, is soft tissue absorption of the X-rays as would be the case in a clinical situation. While the model does not replicate the human jaw wholly, it is an adequate approximation for the purposes of this study.

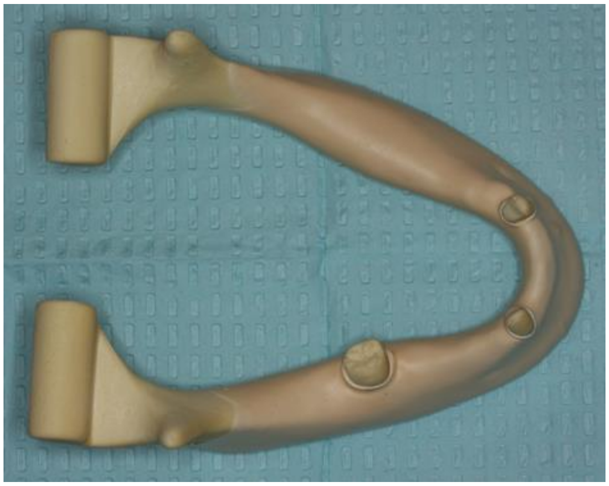

Figure 3: Occlusal view of the model mandible for implant placement

Figure 4: Side view of the model mandible used for implant placement

This model was then scanned in its entirety using a Trios (3shape, Copenhagen, Denmark) intraoral three-dimensional optical scanner. This generated a stereolithography file format commonly referred to as STL.

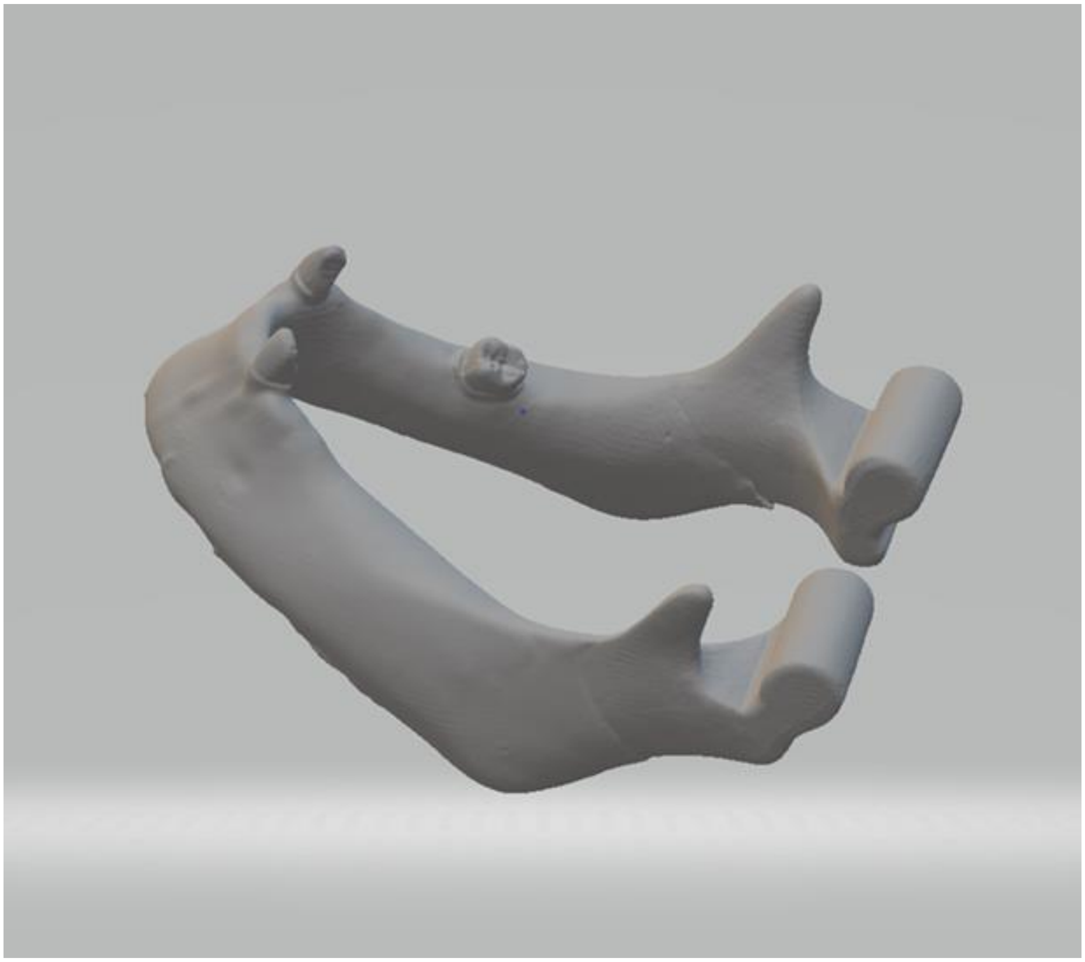

Figure 5: Stereolithography of model mandible generated by the intraoral 3-D scanner

A CBCT image of the model was also acquired using the same Carestream 9300 machine used to obtain the images for part 1 of this study.

Figure 6: Model mandible placed in the Carestream 9300 machine for CBCT acquisition

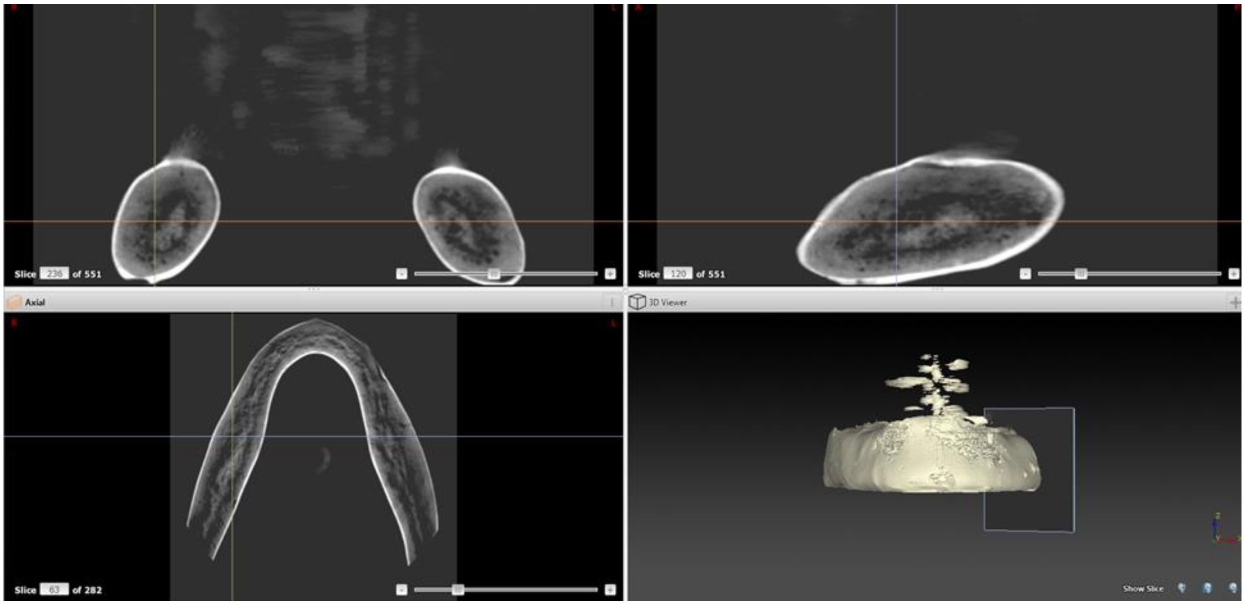

Figure 7: DICOM file of model mandible imported from Carestream 9300

The STL file generated by the scanner and the DICOM file from the Carestream 9300 machine were imported into Blue Sky Plan 4 (BlueSkyBio, Libertyville, USA) virtual implant planning software, which is available for download free of charge through the BlueSkyBio website. Virtual implant consisted to placing two implants in the left side of the model and one implant in the right side of the model. The two implants in left side were virtually placed 5mm from each other. This measurement was taken from the distal shoulder of the mesial implant (Implant #1) to the mesial shoulder of the distal implant (Implant #2) at a line bisecting the centre of each implant in the buccolingual dimension. The implants were also placed parallel to each other. As mentioned earlier, a third implant on the right side of the model was also planned for placement in a position that was directly opposite to the position of the implants on the left side. Straumann 4.1 x 10mm BL (Straumann, Basel, Switzerland) implants were selected in virtual planning as these were frequently placed in the posterior mandible at the UBC Periodontics clinic.

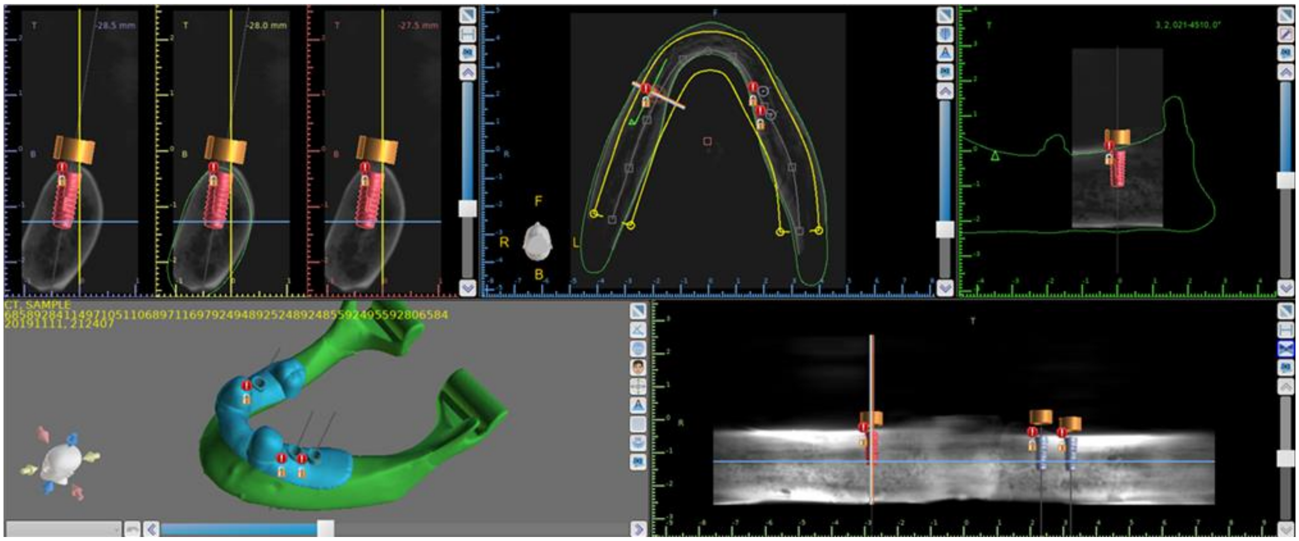

Figure 8: Virtual planning in Blue Sky Plan 4 implant planning software

2.2.2 Placement of Implants

Once virtual planning on Blue Sky Plan 4 was finalized, a virtual surgical guide was fabricated within the software that would allow for a more accurate translation of the virtual plan into reality.

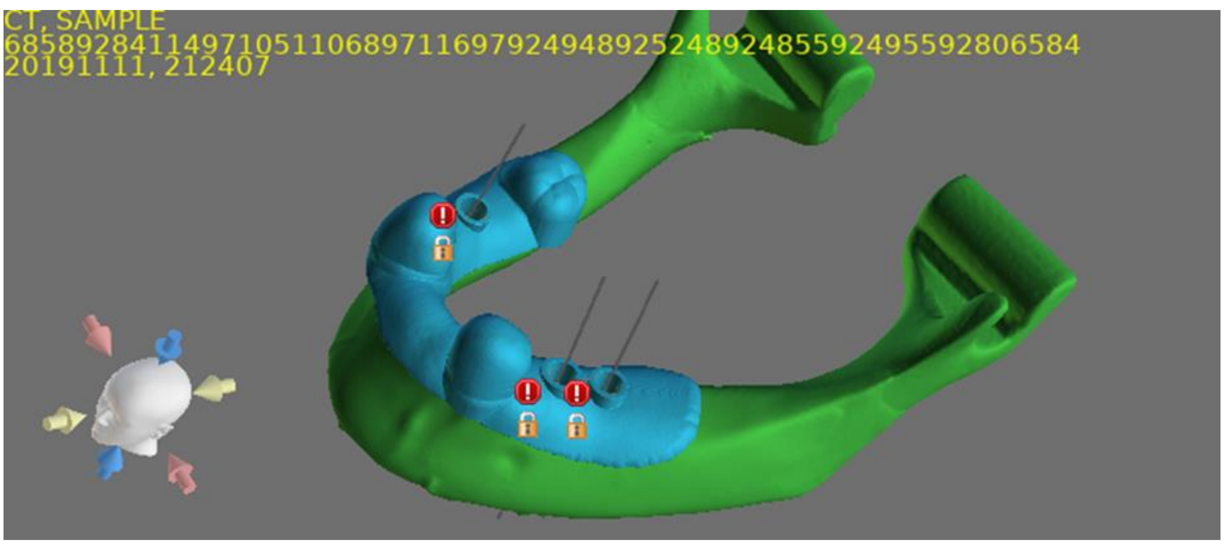

Figure 9: Virtual planning of surgical guide in the Blue Sky Plan 4 software

The STL file for the surgical guide was exported into Formlabs Form 2 3D printer (Formlabs, Medford, USA) via the Preform 3D (Formlabs, Medford, USA) printing software. The 3D printer was used next to fabricate the guide.

Figure 10: Surgical guide after fabrication and processing

The guide was subsequently processed as per the manufacturer's instructions and test-fitted onto the model mandible. No rocking motion of the guide was noted, suggesting that the fit of the guide to the model was precise.

Figure 11: Surgical guide fitted to the model

Two Straumann 4.1mm x 10mm bone level SL implants were placed in the left side of the model as had been decided during virtual planning. The manufacturer's recommended surgical protocol was followed for this procedure.

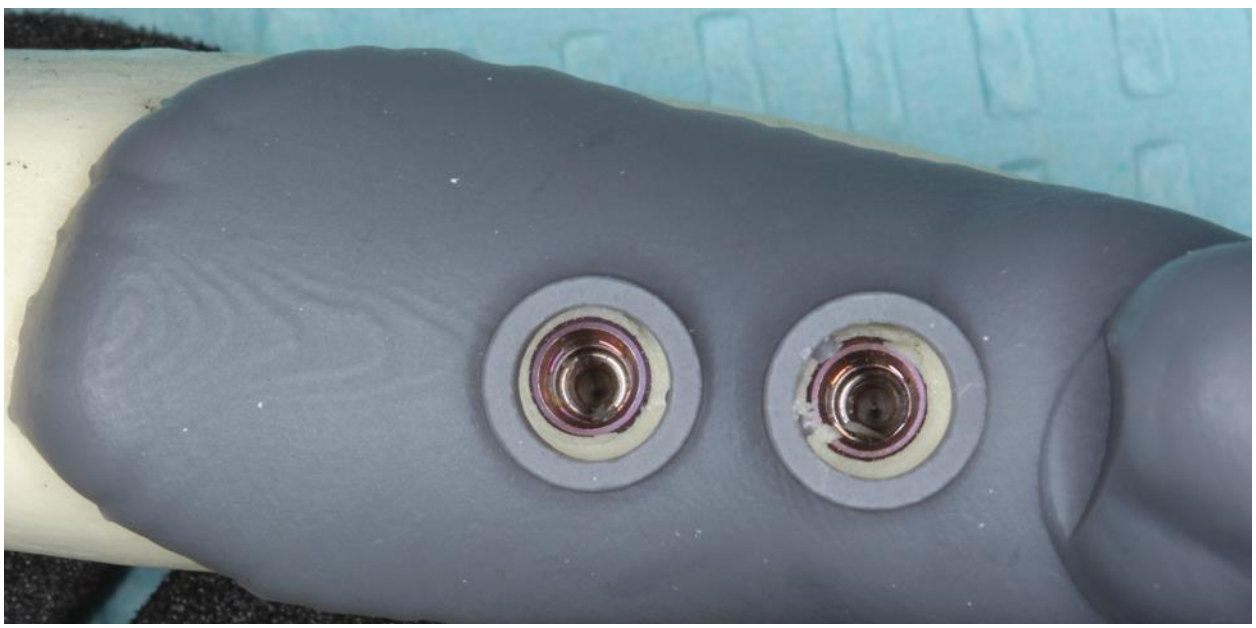

Figure 12: Straumann 4.1x10mm bone level implant placed using the guide

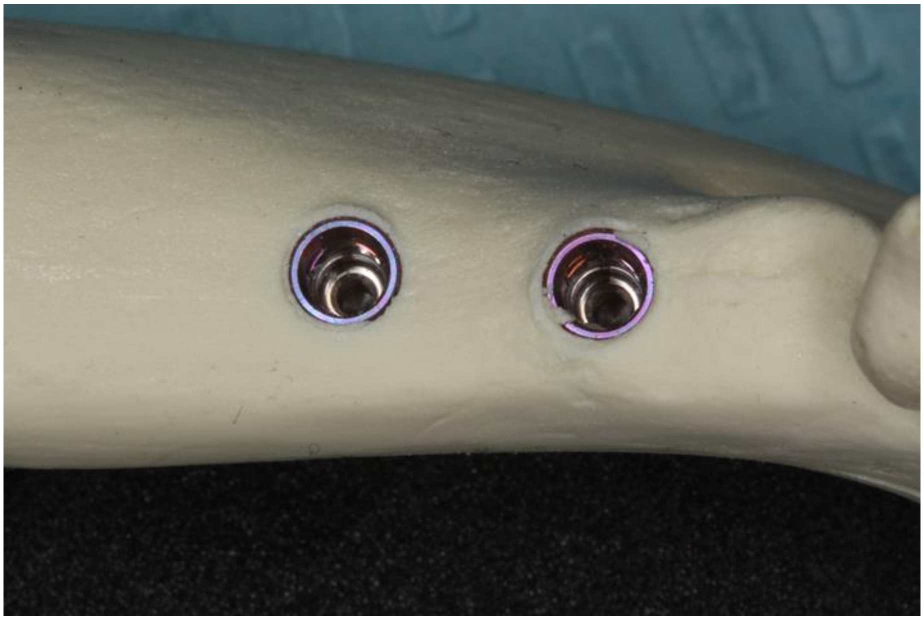

Figure 13: Implant position after removal of guide

Note that both implants were placed to the level of the “alveolar crest” as would be typical in a clinical scenario

2.2.3 CBCT image acquisition

The model mandible was glued to a foam insert that fits precisely into the CBCT machine to ensure that the position of the model did not change within the machine during the subsequent image acquisition and data collection.

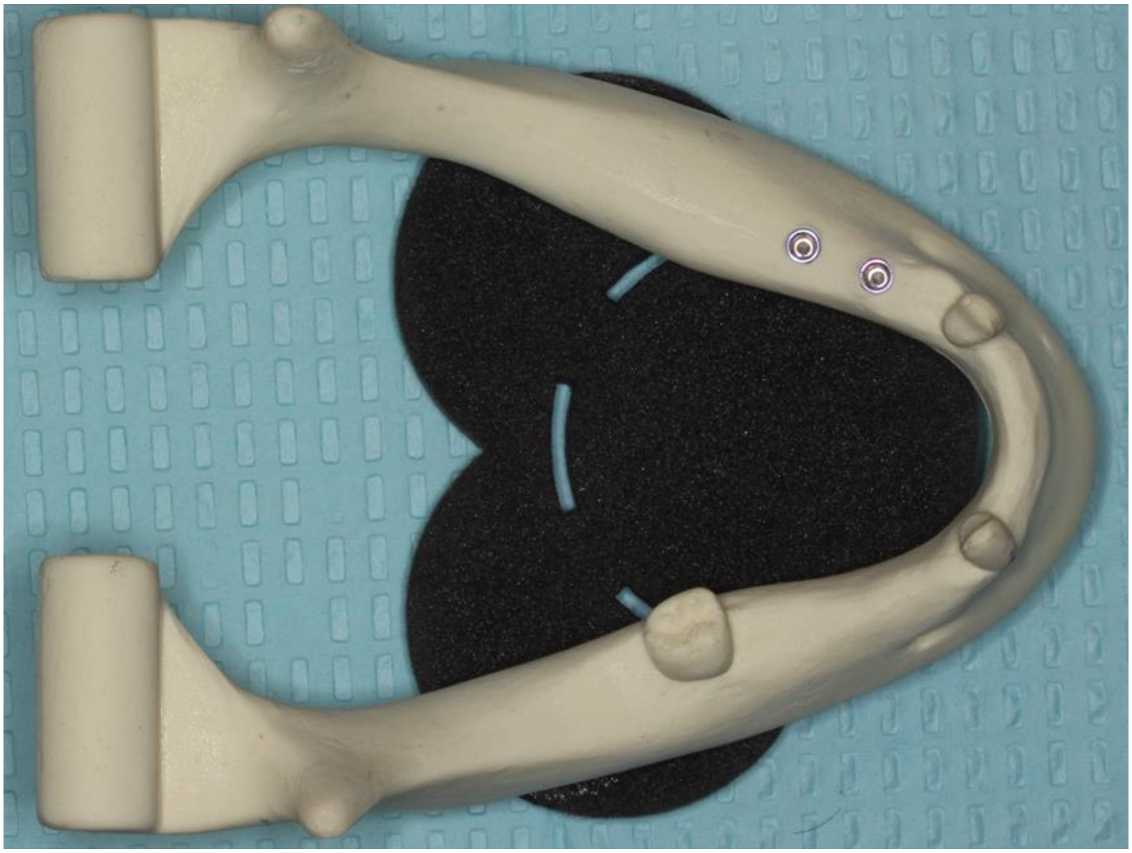

Figure 14: Model glued to foam insert that fits precisely into a platform within Carestream 9300

The model mandible was then placed in the Carestream 9300 machine and a set of images was acquired at the following parameters:

FOV	kvP	mA	Scan time
5x5	90	2	19.96
5x5	90	2.5	19.96
5x5	90	3.2	19.96
5x5	90	4	19.96
5x5	90	5	19.96
5x5	90	6.3	19.96
5x5	90	8	19.96
5x5	90	10	19.96

Table 3: Parameters used for small Field of View scans – varying mA

FOV	kvP	mA	Scan time
5x5	60	5	19.96
5x5	70	5	19.96
5x5	80	5	19.96
5x5	90	5	19.96

Table 4: Parameters used for small Field of View scans – varying kVp

FOV	kvP	mA	Scan time
10x5	90	2	8.01
10x5	90	2.5	8.01
10x5	90	3.2	8.01
10x5	90	4	8.01
10x5	90	5	8.01
10x5	90	6.3	8.01
10x5	90	8	8.01
10X5	90	10	8.01

Table 5: Parameters used for the medium Field of View scans - varying mA

FOV	kvP	mA	Scan time
10x5	60	4	8.01
10x5	70	4	8.01
10x5	80	4	8.01
10x5	90	4	8.01

Table 6: Parameters used for medium Field of View scans - varying kVp

The manufacturer's recommended imaging parameters for a low resolution small FOV scan are 5mA, 85kVp with an exposure time of 12 seconds. The patient is exposed to 358 milli Gray of radiation during this scan. For the high resolution small FOV scan, the exposure time is increased to 19.96 seconds while the tube current is unchanged and tube voltage is set to 84kVp. This exposes the patient to an additional 257 milli Gray of radiation. The recommended parameters for a medium FOV scan are 4mA, 90kVp, and an exposure time of 8.01s, which exposes the patient to a total radiation dose of 486 milli Gray. The Carestream software at UBC is restricted to low resolution images for all FOVs larger than the 5x5 small FOV.

For the first set of CBCT images, a 5x5 FOV was utilized. The kVp and scan time were held constant at 90kV and 19.96 seconds, respectively, while the mA was varied. A second set of images was then acquired holding the mA and scan time constant at 5mA and 19.96 seconds, while the kVp was manipulated. The mA values were varied in the increments allowed by the Carestream software while kVp values were varied in increments of 10 from the lowest to the highest possible allowable limit.

This process was then repeated for the 10x5 FOV. Notable difference between the 5x5 and the 10x5 FOVs is that the scan time is set at 8.01s for 10x5 images whereas it is 19.96s for the 5x5 images. Furthermore, the voxel size is 0.09mm for the 5x5 FOV whereas its set to 0.18mm for the medium FOV.

Upon completing these scans, a third Straumann 4.1mm x 10mm bone-level SL implant was placed in the right side as previously planned in the Blue Sky Plan 4 software. The same guide used in initial implant placement on the left side was used to place this third implant. The same surgical protocol recommended by the manufacturer was followed. Both 5x5 and 10x5 scans were then repeated using the same parameters mentioned earlier. The objective of this part of the experiment was to evaluate whether scatter and metal artifacts from an additional implant on the opposite side would influence the measurements between the two implants that were placed initially.

The whole experiment was then repeated in the exact same sequence for a second model mandible. Our goal was to obtain a more robust data set.

Sample images can be found in Appendix B of this document.

Figure 15: Image acquisition after placement of 3rd implant on the right side

2.2.4 Measurements and Data Collection

All images acquired through the Carestream 9300 machine were reviewed in the accompanying software. This is the same software used by all graduate and undergraduate students at UBC Faculty of Dentistry for reviewing and recording diagnostic information for all CBCT images.

When studying the images, the same monitor was used throughout. No adjustments were made to brightness, contrast etc. in either the viewing software or to the monitor. Three measurement were made in both the axial and sagittal planes.

Measurements were taken to the nearest tenth of a millimeter at all predetermined landmarks on the implant body. In order to standardize the measurements across all samples, measurements were taken at the same locations in both the axial and sagittal planes. To obtain measurements in the sagittal plane, projection taken through the midpoints of the two adjacent implants was utilized for all images. The resulting two-dimensional image was used to perform the measurements employing the measuring tool within the software. The first measurement was taken at the level of the implant crest. It extended from the distal aspect of the implant placed mesially (Implant #1) to the mesial aspect of implant placed distally (Implant #2). This measurement was at the level of the implant crests. The second measurement was taken at the level of the implant threads directly adjacent to the point where the internal screw channel within the implant body terminated. The third measurement was taken at the level of the second to the last thread on the implant body. The last thread of the implant body was not used to conduct the measurements as its depth is much smaller than the other threads and it was obscured in the some of the CBCT images. The second and third measurements were taken between the crests of the respective threads.

Mechanisms within the Carestream 9300 software were employed to standardize all measurements in both planes in order minimize the measurement error as much as possible. The Carestream software has several tools that allow the user to manipulate and review all the two-dimensional projections that make up the three-dimensional image reconstruction. For example, within the sagittal plane, a line can be dragged in superior-inferior or coronal-apical direction in order to view the corresponding slices in the axial plane. The axial plane also has a similar tool that allows the user to move in the left-right direction to view the corresponding slices in the sagittal plane. These built-in “lines” within the Carestream software were used to ensure that the three measurements in both planes were parallel to each other.

Within the sagittal plane, the three measurements were considered to be parallel if the reference line in the program completely overlapped all three measurements without any discrepancy when manipulated in coronal-axial direction or vice versa. This is illustrated in the image below.

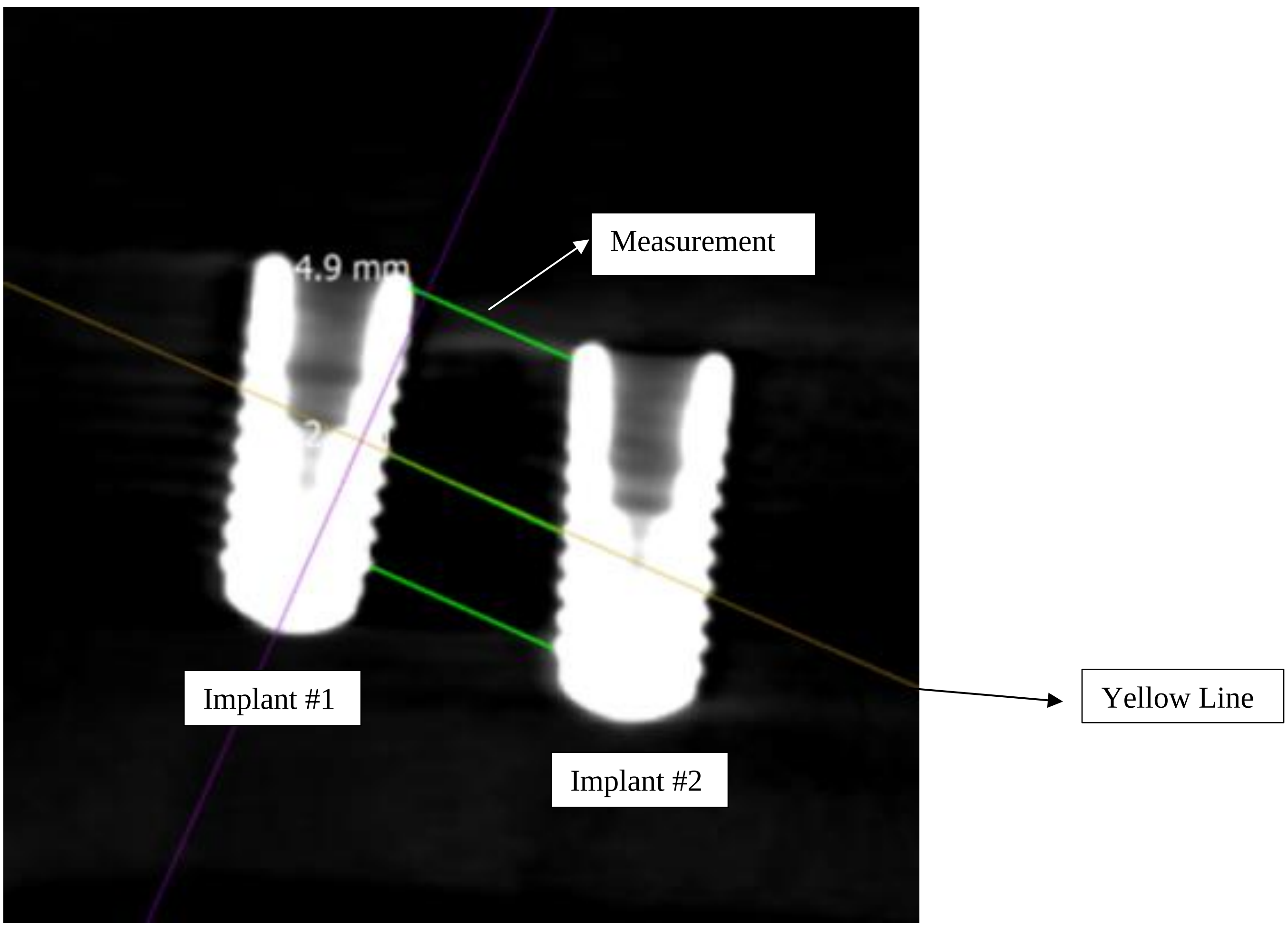

Figure 16: Parallelism between the reference line and measurements

Note: The yellow line in the image above, used to move through the projection in the apical-coronal direction, was used to ensure that the three measurements taken are completely parallel to each other. If there was a complete overlap between the yellow line and the three green lines that represent the three different measurements, then we can assume parallelism between the three measurements with a high degree of confidence.

A similar quality control methodology was used for measurements in the axial plane. Axial measurements were taken at the same location as the measurements in the sagittal plane. When the reference line in the sagittal plane was overlapping each individual measurement completely, the image was switched to the axial view. This means that we were viewing the same projection in the axial view as we were in the sagittal view where the measurement was taken. In the axial image, measurements were taken from the most distal point on implant#1 to the most mesial point on implant #2 along a reference line that bisected both implants through centre of their bodies. A complete overlap of the reference line and the measurement line was ensured to standardize the measurements as was done with the measurements in the sagittal plane. This is illustrated in the image below.

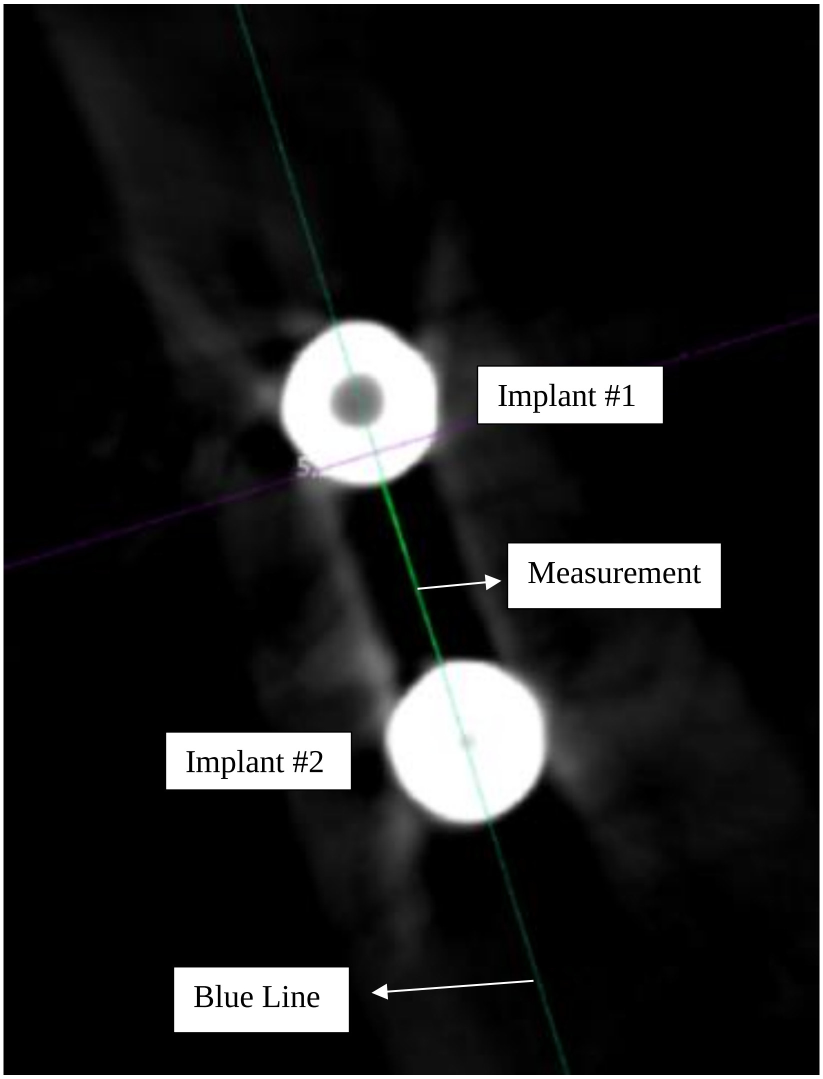

Figure 17: Axial view illustrating the overlap between the reference line and measurement

The green line in the image above represents the distance measurement taken between the two implants. The blue line built into the software, completely bisects the implants at their center and overlaps the green measurement line completely. This was done to obtain standardization and minimize error.

2.3 Statistical Analysis

Comparisons were made between the various data sets. Specifically, for both the small and medium fields of view, findings were compared separately when mA and kV were held constant.

Furthermore, these findings were compared within each FOV when a third implant was added. Additionally, the small and medium FOVs were compared with each other for both two and three implant data sets. A two-way ANOVA statistical test was performed to determine whether the observed differences reached statistical significance. This statistical test was performed in GraphPad Prism 8 software. Differences were considered to be statistically significant when $P<0.05$ and two-tailed.

We also performed Tukey's test for post-hoc analysis as we felt that further analysis beyond a two-way ANOVA was needed. There was value in comparing measurements within each imaging parameter between the different values being studied. For example, when mA values were varied, we felt that it was important to compare the different measurements obtained within a specific mA value with the measurements obtained in each of the other mA values. In this manner, we could illicit any differences present between the measurements at specific mA and kVp values beyond the overall comparison of two-way ANOVA.

Chapter 3: Results

3.1 CBCT Audit from Jan. 2015 to Aug. 2018

Between the period of January 2015 and August 2018, a total of 704 CBCT prescriptions were made and audited in electronic patient record database at the UBC Faculty of Dentistry. Majority of these prescriptions originated from the Graduate Periodontics (45%) and Graduate Endodontics (38%) programs. A small minority of the CBCTs were prescribed by the Graduate Prosthodontics program (10%) while the DMD (4%) and Graduate Orthodontics (3%) programs accounted for even a smaller proportion of the prescriptions. There were no prescriptions from the Graduate Pedodontics department, and 2 prescriptions were through faculty practice or other miscellaneous sources.

Program	Scans
Periodontics	321 (45%)
Endodontics	266 (38%)
Prosthodontics	69 (10%)
Orthodontics	19 (3%)
Pedodontics	0 (0%)
DMD	27 (4%)
Other	2 (0%)
Total	**704**

Table 7: Number and percentages of CBCTs taken by all disciplines at UBC

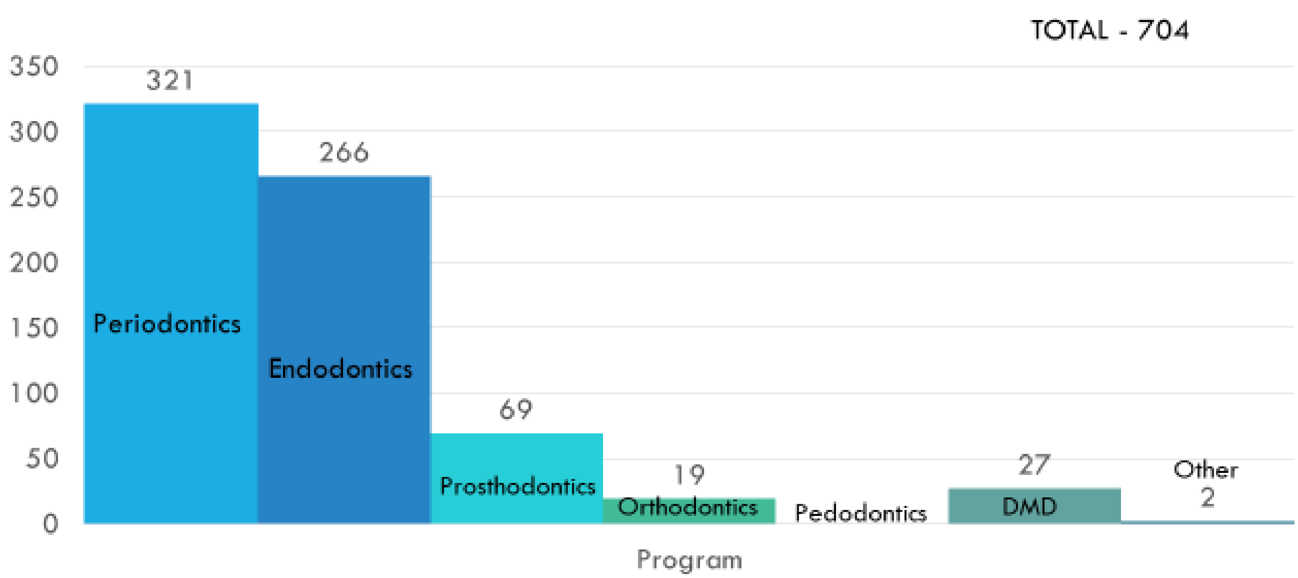

Figure 18: Number of CBCTs taken by each discipline

The prescriptions from the Graduate Periodontics and Prosthodontics programs were reviewed separately from the other specialties with an emphasis on implant planning. Out of the 321 cases prescribed by the Graduate Periodontics Program, 313 were for the purposes of implant treatment planning. Specifically, the referrals for CBCT were made to assess the bone height and width, bone quality or to assess the proximity of vital structures (inferior alveolar canal, maxillary sinus etc.) before implant placement OR follow up of maxillary sinus augmentation or lateral ridge augmentation procedures. For the Graduate Prosthodontics program, all 69 prescriptions were for the sole purpose of implant treatment planning. In total, 382 CBCT scans were prescribed for the purposes related to implant treatment planning between January 2015 and August 2018 at the UBC Faculty of Dentistry. In the Graduate Periodontics program, a small percentage of the scans were taken to assess suspected pathology (4) and to evaluate the position of an impacted canine or third molar for the purpose of either removal or exposure (4).

Reason for Prescription	Scans
For placement of implants, to assess the bone width and bone quality and to assess the proximity of vital structures (Inferior alveolar canal, maxillary sinus etc.) before implant placement OR Follow up of Maxillary sinus augmentation or Lateral ridge augmentation	313 (98%)
Pathology	4 (1%)
Impaction (canine or 3rd molar)	4 (1%)

Table 8: CBCT prescriptions in the Graduate Periodontics program

Reason for Prescription	Scans
For placement of implants, to assess the bone width and bone quality and to assess the proximity of vital structures (Inferior alveolar canal, maxillary sinus etc.) before implant placement	69 (100%)

Table 9: CBCT prescriptions in the Graduate Prosthodontics program

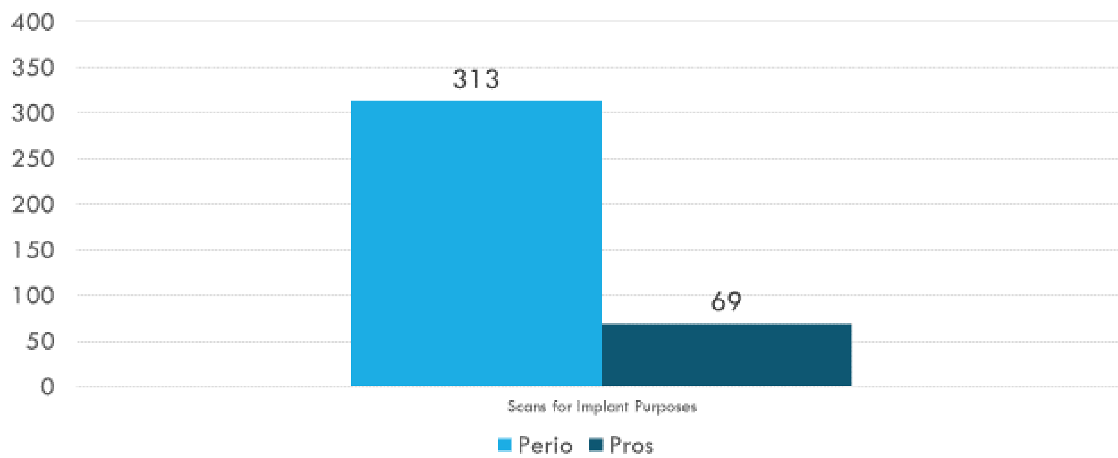

Figure 19: Implant related prescriptions in Graduate Periodontics and Prosthodontics programs

For the patients prescribed CBCTs in the Graduate Periodontics program, the gender distribution between males (160) and females (161) was almost equal. In the Graduate Prosthodontics Program, however, majority of the prescriptions were in the male gender (40) as compared to the female gender (29).

Gender	Scans
Male	160 (50%)
Female	161 (50%)

Table 10: Number and percentages of males and females in the Graduate Periodontics program

Gender	Scans
Male	40 (58%)
Female	29 (42%)

Table 11: Number and percentages of males and females in the Graduate Prosthodontics program

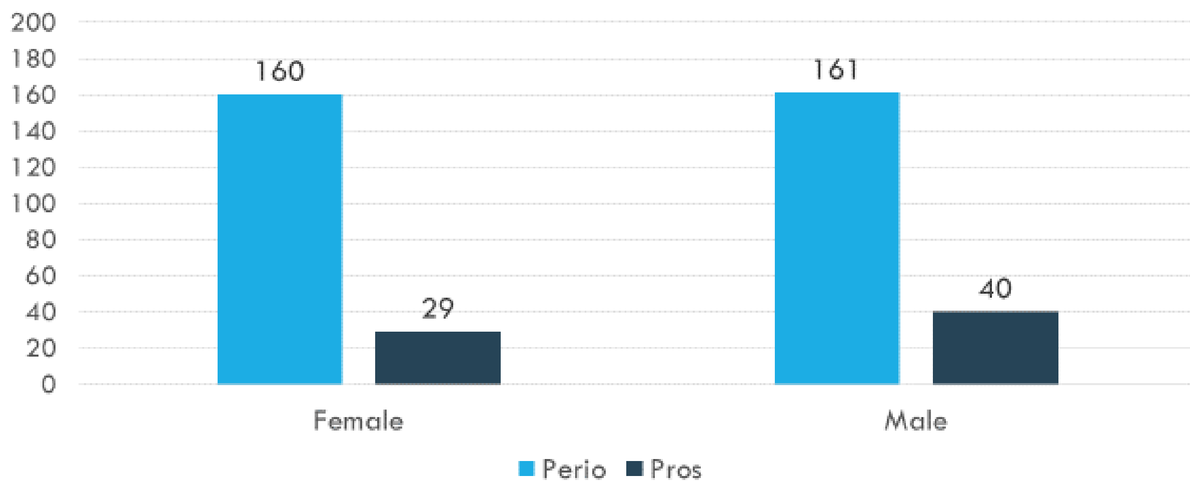

Figure 20: Comparison of males and females for CBCT in the Periodontics and Prosthodontics programs

Majority of the patients that had a CBCT prescribed in the Graduate Periodontics and the Prosthodontics departments were between the ages of 41 and 80. A more comprehensive breakdown of age as it relates to CBCT prescriptions in both departments can be found in the figure below.

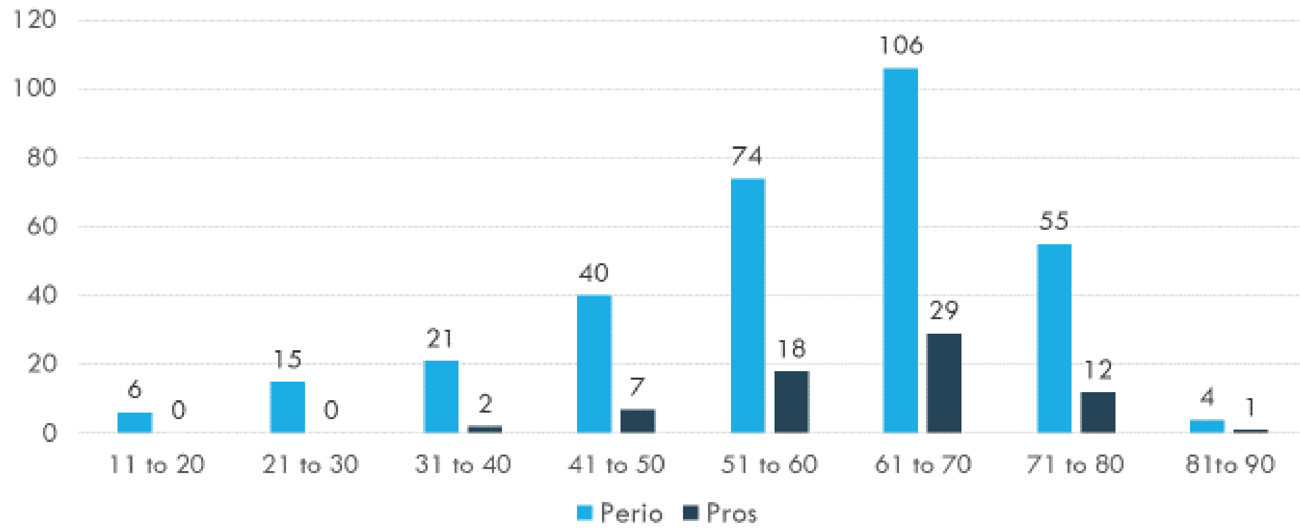

Figure 21: Age distribution of CBCT Prescriptions in the Periodontics and Prosthodontics programs

Majority of the cases (161) prescribed in the Graduate Periodontics program were low resolution, small (5x5) FOV. Majority of cases (45) prescribed in Graduate Prosthodontics program were medium (10x5) FOV. A further characterization of the cases by their respective FOVs in both the Graduate Periodontics and Prosthodontics programs can be seen in the tables and figure below.

FOV (Resolution)	Scans
5x5 (low)	161 (50%)
5x5 (high)	12 (4%)
5x10 (low)	105 (33%)
8x8 (low)	18 (5%)
10x10 (low)	25 (8%)

Table 12: Fields of view in the Graduate Periodontics program

FOV (Resolution)	Scans
5x5 (low)	13 (19%)
5x5 (high)	0 (0%)
5x10 (low)	45 (65%)
8x8 (low)	3 (4%)
10x10 (low)	8 (12%)

Table 13: Fields of view in the Graduate Prosthodontics program

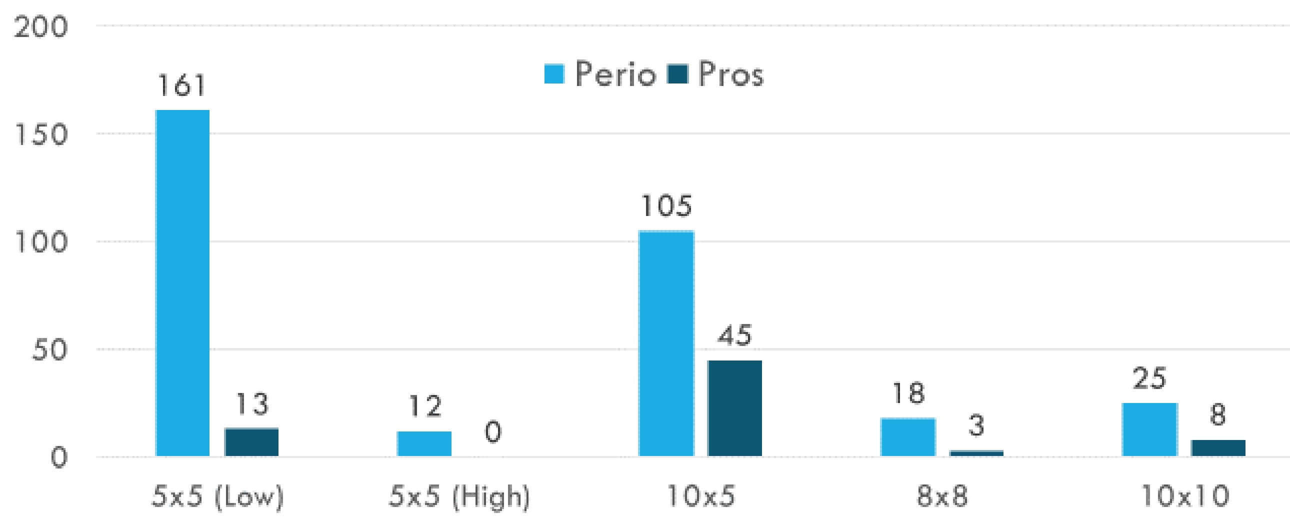

Figure 22: Fields of view comparison between the Graduate Periodontics and Prosthodontics programs

Distribution of the CBCT prescriptions as it relates to the sites i.e. maxilla, mandible or both is listed in the tables below for both the Graduate Periodontics and Prosthodontics programs.

In the Periodontics department, majority of the scans were for the maxilla whereas in the Prosthodontics department, the distribution of scans prescribed for the maxilla or the mandible was more even.

Site	Scans
Max	157 (49%)
Mand	121 (38%)
Both	43 (13%)

Table 14: Location of scans in the Graduate Periodontics program

Site	Scans
Max	30 (43%)
Mand	28 (41%)
Both	11 (16%)

Table 15: Location of scans in the Graduate Prosthodontics program

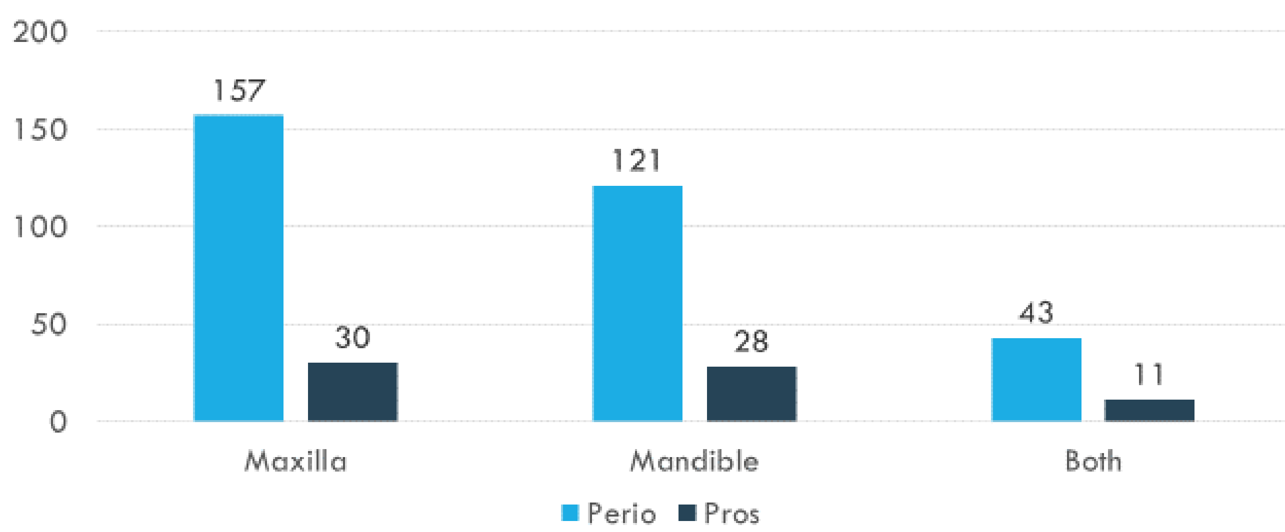

Figure 23: Comparison of sites between the Graduate Periodontics and Prosthodontics Programs

3.2 Compliance with published recommendations

In the Graduate Periodontics department, 297 out of 313 prescriptions had a conventional two-dimensional image prior to CBCT request for implant planning. This equals to 95% of the total prescriptions having a conventional image prior to a CBCT. When further evaluating the type of two-dimensional imaging that was present, 87 (29.3%) of the images were panoramic radiographs, 199 (67.0%) were peri-apical radiographs and 11 (3.7%) were bitewings.

Figure 24: Conventional image prior to CBCT in the Graduate Periodontics program

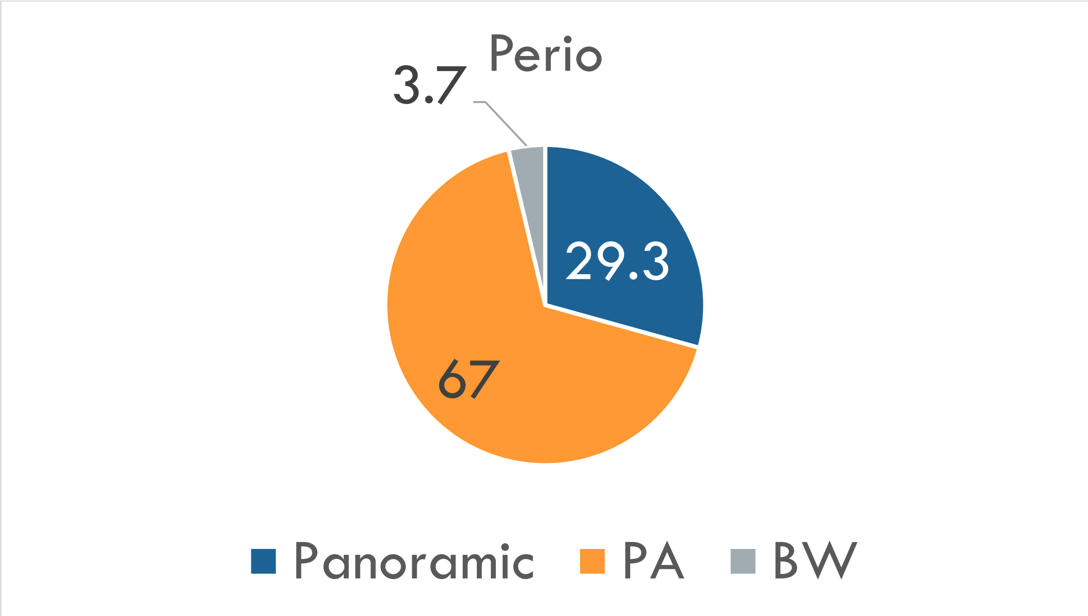

Figure 25: Type of 2-D image prior to 3-D image in the Graduate Periodontics program

In the Graduate Prosthodontics department, 65 out of 69 prescriptions made for the purposes of implant planning had a conventional image prior to the reacquisition request. This amounts to 94% of the total prescriptions having a two-dimensional image prior to the acquisition of cross-sectional imaging. When further evaluating the type of two-dimensional imaging that was present, 30 (43.5%) of the images were panoramic radiographs and 39 (56.5%) were peri-apicals.

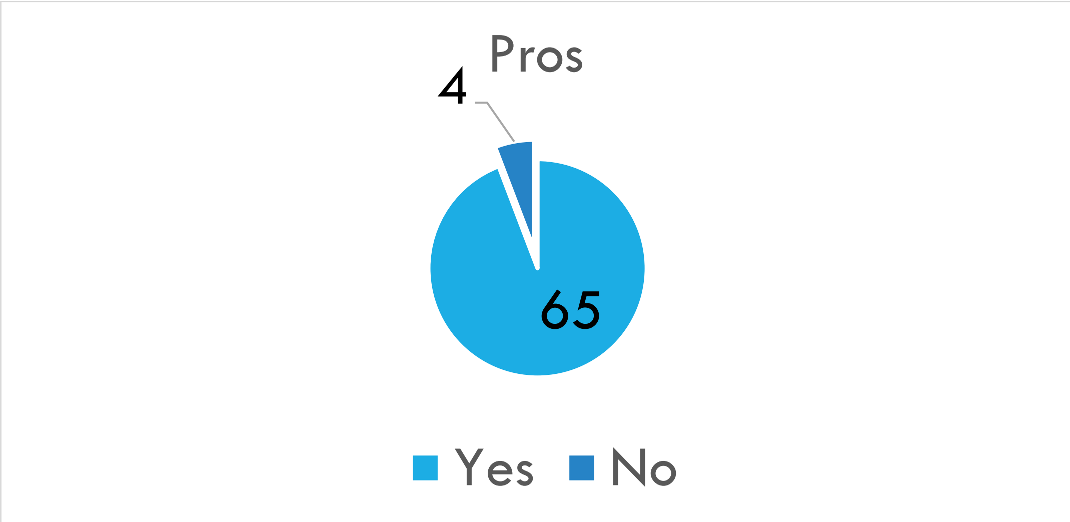

Figure 26: Conventional image prior to CBCT in the Graduate Prosthodontics program

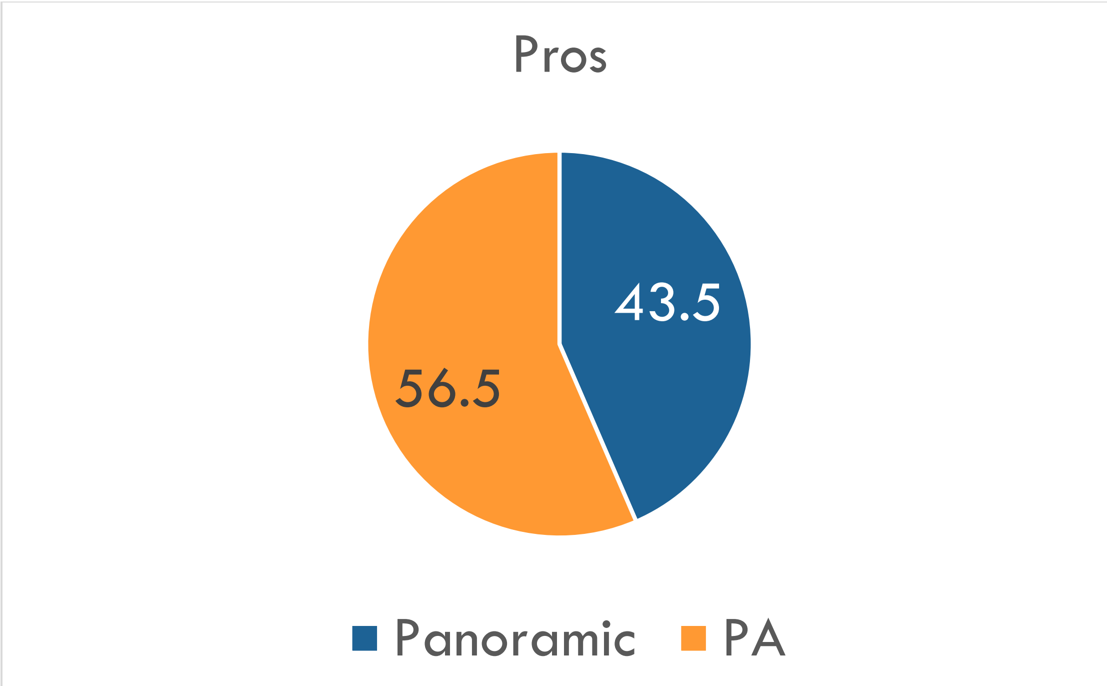

Figure 27: Type of 2-D image prior to 3-D image in the Graduate Prosthodontics program

From the 382 total prescriptions made in both the Graduate Periodontics and Prosthodontics programs for the purposes of implant treatment planning, 84 were repeat prescriptions. In other words, 84 patients were exposed to two scans in the same region. The second prescription in all 84 cases was for the purpose of evaluation of the potential implant site post lateral ridge or sinus augmentation. No patient was exposed to three or more scans at the same site within the time period studied.

3.3 Manipulation of CBCT parameters

3.3.1 Measurements between implants

The data tables for the measurements can be found in Appendix C section of this document. The difference in the measured distance between the two implants ranged from 0mm to 1.6mm as the mA and kVp values were varied. The tables from the 2-way ANOVA comparison for the various parameters can be located in Appendix D.

3.3.2 Relationship between mA and measurements for small and medium FOVs (2 implants)

Manipulation of the mA values did not result in a statistically significant differences in measurements between two implants overall in either FOV with P-values being 0.4561 and 0.6260 for small and medium FOVs, respectively. However, further comparison between specific mA values while holding kVp constant did reveal both statistically and clinically significant results (Figures 28 and 29). For example, in the small FOV scans, when comparing the measurements at 2mA and 10mA, there was a mean difference of 1.1mm in measurements at crestal, mid and apical levels (P value <0.05). This was both statistically and clinically significant. All the statistically significant results are listed in the figures below for both FOVs.

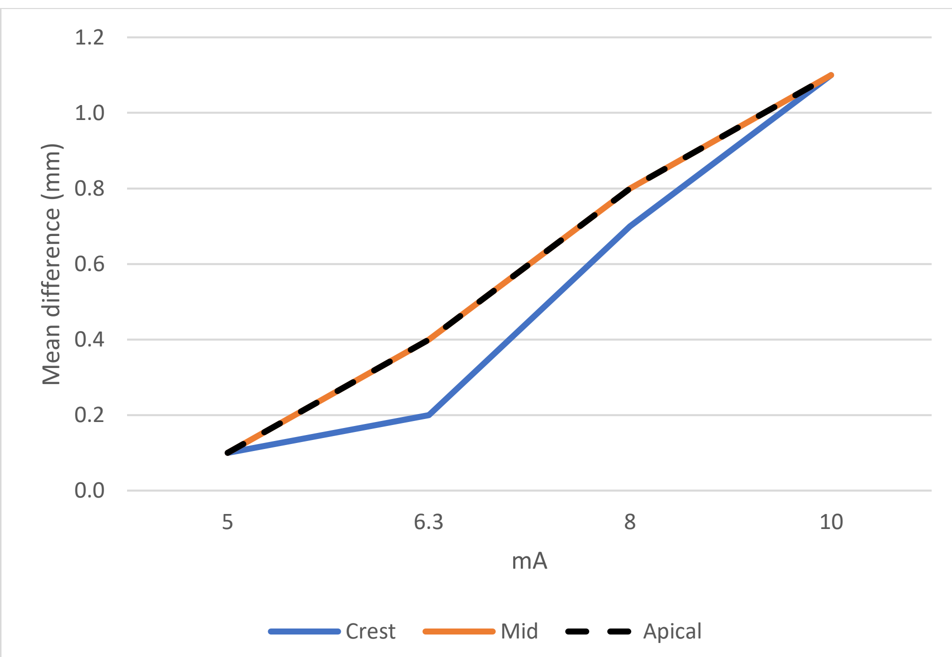

Figure 28: Mean difference in implant distance at various mA values compared to 2mA for small FOV

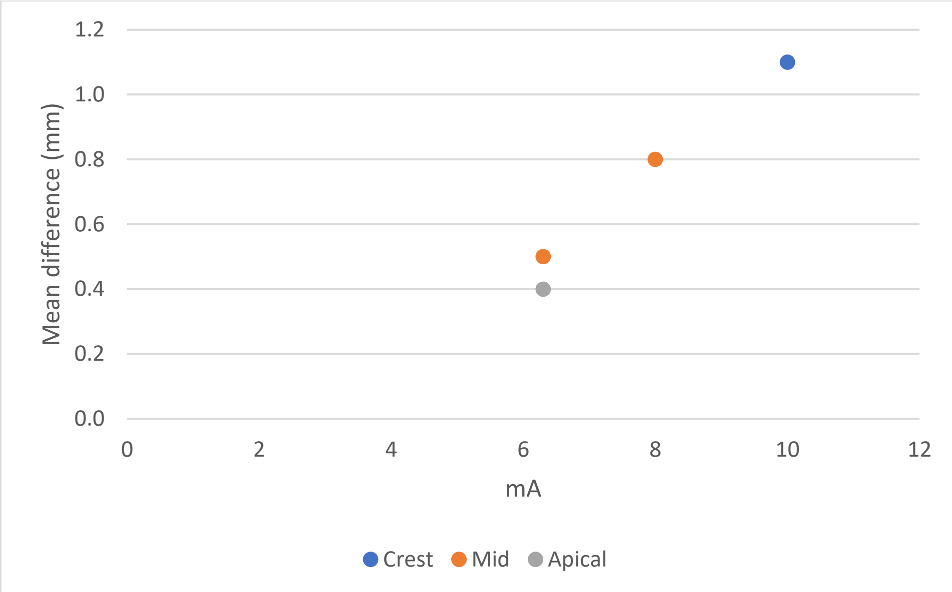

Figure 29: Mean difference in implant distance at various mA values compared to 2mA for small FOV

3.3.3 Relationship between kVp and measurements for small and medium FOVs (2 implants)

Like the results obtained for varying mA values, changing the kVp values did not result in a statistically significant differences in measurements between two implants overall in either FOV. The respective P-values for this comparison for the small and medium FOVs were 0.4499 and 0.4555. However, when the data was examined more closely, statistically significant differences could be found between measurements when comparing specific kVp values (Tables 16 and 17). All statistically significant results are listed in the tables below for both FOVs.

Comparison	Mean Difference (mm)		
	Crest	Mid	Apical
60kVp vs. 80kVp	-	0.1	-
60kVp vs. 90kVp	-	0.3	0.2
70kVp vs. 90kVp	0.2	-	0.1
80kVp vs. 90kVp	-	-	0.1

Table 16: Statistically significant differences for small field of view scans with 2 implants comparing kVp

Comparison	Mean Difference (mm)		
	Crest	Mid	Apical
60kVp vs. 80kVp	-	0.1	0.1
60kVp vs. 90kVp	-	-	0.1
70kVp vs. 80kVp	0.1	0.1	-
70kVp vs. 90kVp	0.2	0.1	0.1
80kVp vs. 90kVp	-	-	0.1

Table 17: Statistically significant differences for medium field of view scans with 2 implants comparing kVp

3.3.4 Comparing measurements between small and medium FOV scans with 2 implants

When measurements between implants were compared with respect to the FOV, no statistically significant differences could be found overall between the small and medium fields for all mA and kVp value studied. The P-values for the comparison between small and medium FOVs for varying mA and kVp were 0.5076 and 0.4072, respectively. However, certain measurements listed in Table 18 met the threshold of statistical significance (P-value <0.05) for the listed mA values. The mean difference between measurements did not exceed 0.1mm for each of the mA values.

mA	Mean difference (mm)		
	Crest	Mid	Apical
2.5	-	0.1	-
3.2	-	-	0.1
5	0.1	0.1	-
6	0.1	0.1	-
10	0.1	0.1	-

Table 18: Statistically significant differences between small and medium fields of view at varying mA values

3.3.5 Addition of third implant

The addition of third implant to the opposite did not result in statistically significant changes in measurements when comparing the results within each field of view or when comparing the results between small and medium FOVs for both varying mA and kVp values (Table 19).

Comparison	P-value
2 vs 3 implants for small field of view with varying mA	0.4479
2 vs 3 implants for small field of view with varying kVp	0.3877
2 vs 3 implants for medium field of view with varying mA	0.5133
2 vs 3 implants for medium field of view with varying kVp	0.4077
small vs medium fields of view with 3 implants for varying mA values	0.2753
small vs medium fields of view with 3 implants for varying kVp values	0.2627

Table 19: P-values for various comparisons after addition of a third implant

Chapter 4: Discussion

4.1 CBCT Audit

Along with clinical examination, radiography forms an essential part of diagnosis, treatment planning and subsequent treatment outcomes. Although two-dimensional imaging may be adequate for many clinical scenarios in the specialty of periodontics, cross-sectional imaging has become the standard of care for implant treatment planning. The use of cross-sectional imaging before placement of dental implants was first recommended by Schwarz et. al in 1987. Since then, advances in technology have allowed the dental practitioner to obtain cross-sectional images that are of better quality while exposing the patient to a lower radiation dose. It’s smaller size, lower cost, superior spatial resolution and reduced radiation dosage has led to an increase in popularity of CBCT in comparison to planar CT, specifically in the field of dentistry (Watanabe et. al 2019).

CBCT offers many advantages when considering the discipline of implantology. It allows for the precise visualization and location of vital anatomic structures in three dimensions so that a safe distance can be maintained from the final implant location. This can avoid potential invasion of structures such as the inferior alveolar nerve canal, lingual artery, submandibular fossa and maxillary sinus and the accompanying complications caused by such violation (MacDonald, 2011). The clinician can select the size, number and site of implants prior to surgery based on the CBCT. The entire surgery can be virtually planned well in advance in implant treatment planning software, making the execution much easier. The location of the implants, surrounding vital structures and prosthetic requirements can all be accounted for well ahead of the surgical procedure itself (D’Haese et. al 2017). This virtual planning can be communicated with colleagues from other disciplines and the patient as necessary. It can also be translated into the patient's oral cavity through the fabrication of a surgical guide. Evidence has shown that accuracy of implant placement can be increased through guided surgery, hence its gain in popularity among clinicians over the last few years (Younes et. al 2018). Virtual planning and guide fabrication would not be possible without the advent of CBCT. Furthermore, CBCT can reveal information about whether sinus or later ridge augmentation will be required prior to implant placement. This information cannot be easily extracted through conventional radiography and/or clinical examination. Given all these advantages, it is not surprising that a significant number of CBCT scans were prescribed in the Graduate Periodontics and Prosthodontics department at the UBC Faculty of Dentistry for implant treatment planning. Although all specialty programs were audited, the focus of this study was on the Graduate Periodontics and Prosthodontics programs at UBC. The CBCT audit revealed that majority of the scans in the Graduate Periodontics department and all the scans in the Graduate Prosthodontics department were prescribed for the purposes of implant related procedures i.e. to assess bone quantity and quality, relation to vital structures or site-evaluation post-sinus or later ridge augmentation (Tables 8 and 9). Only 2% of the scans were prescribed for further evaluation of pathology and canine or third molar impaction in the Graduate Periodontics department. This is in line with the type of procedures that are performed in these specialties. It is important to note that the Graduate Prosthodontics department does not perform any surgical implant placement. So, although Graduate Prosthodontics residents prescribe CBCT scans, these patients are then referred to the Graduate Periodontics residents. Virtual treatment planning is usually a joint effort between the two specialties but the surgical procedures themselves are performed by the periodontics residents.

Field of view characterizes the anatomical region in the patient that will be irradiated during the CBCT acquisition process and will therefore be included in the final CBCT volume. The clinician must decide on the optimal FOV prior to image acquisition based on the clinical indications. In general, the smallest FOV that would yield the required diagnostic information should be selected (MacDonald 2020, Page 617). A small FOV was selected 54% of the time in the Graduate Periodontics program (Table 12). This usually corresponds to cases with either single or two-to-three adjacent implants as part of the treatment plan. Most of these patients are largely dentate with only a few missing teeth and with treatment plans that are uncomplicated i.e. single implant supported crown or small span PFDPs. Approximately 4% of the total prescriptions in Graduate Periodontics Program were the small FOV but with high spatial resolution (Table 12). These prescriptions are concentrated in later part of the audit i.e. in 2018. This reflect a philosophical shift within the program. It was decided that the low-resolution images are sometimes inadequate in displaying the finer details such as the border of the inferior alveolar nerve canal. Rather than exposing the patient multiple times in case a deficient image is obtained, it was decided that the program will prescribe high resolution scans for the small FOV. Approximately a third of CBCT scans (Table 12) in the Graduate Periodontics Program were medium FOV. These are generally indicated when multiple implants are required that are distributed around a single jaw or when guided surgery is planned from the beginning. 5% and 8% of the scans were the 8x8 and 10x10 FOVs, respectively. These signify more complex treatment plans where the treatment plan involves placement of implants in both arches.

In the Graduate Prosthodontics program, a vast majority of the prescriptions were for medium and large FOVs (Table 13). Only 19% of the prescriptions indicated a small FOV (Table 13). There are two main reasons for this discrepancy. First, due to the nature of the specialty itself, majority of the patients who present to the program require complex treatment. Patients seeking treatment in the Graduate Prosthodontics program are usually referred from either the DMD program or from external general dentist providers who have deemed the treatment to be too complicated for their own scope of practice. These patients are either missing several teeth, in terminal dentition or are completely edentulous. Treatment for these patients consists of disperse placement of multiple implants in the maxilla, mandible or both jaws. Therefore, larger FOVs are usually required for implant treatment planning. Even when the prosthodontic treatment plan is limited to placement of single unit implant supported restorations, these cases usually involve placement of an implant in the esthetic zone such as the anterior maxilla. To successfully treat a single missing tooth in the esthetic area has been described as potentially one of the most complicated clinical situations from both a surgical and restorative prospective (Schoenbaum 2018, page 4). Precise implant placement becomes more important in these cases as it will have great impact on restorative treatment. Therefore, the preference of the prosthodontic residents has been for the periodontology residents to perform the surgery guided. Guided surgery involves merging radiographic data with the optical intraoral scan (Schoenbaum 2018, page 41). In general, a full arch CBCT is required to have enough widely spaced landmarks that can be merged with the intraoral scan. A surgical guide that straddles the entire arch is often fabricated for stability and minimizing error that can result from an unstable guide. This is the second reason why a large proportion of the prescriptions originating from the Graduate Prosthodontics program are medium and large FOVs.

There was an equal distribution of CBCTs with respect to gender in the Periodontics program (Table 10) whereas more male patients had a CBCT scan prescribed in the Prosthodontics programs than female patients (Table 11). Although the prevalence of complete edentulism has been reported to be similar among both males and females, the prevalence of tooth loss is 46.7% in males vs 38.1% in females according to Health Canada data from 2010 (Russell et. al 2013). This may explain the higher number of male patients presenting in the Prosthodontics department for implant treatment.

In both the Periodontics and Prosthodontics programs, more scans were prescribed for the maxillary arch than the mandibular arch (Tables 14 and 15). However, the discrepancy in the Periodontics was much greater than Prosthodontics. Patients presenting to the Periodontics program not only present for implant treatment for edentulous spaces but also for management of periodontal disease. Furthermore, many patients seeking implant treatment are unaware or undiagnosed for the presence of periodontitis and require disease management prior to implant therapy. It has been well established that the most frequent teeth lost due to periodontal disease are the maxillary molars (Hirschfeld et. al 1978, Upadhyaya et. al 2009). This can explain why there were more CBCTs prescribed for the maxilla, especially in the Periodontics department.

In both departments, CBCTs were most frequently prescribed for patients in the sixth decade of their lives (Figure 23). This is not surprising as patients are more likely to lose teeth with increasing age. In the latest National Health and Nutrition Examination Survey (NHANES), it was reported that adults between the ages of 50-64 have at least 3 fewer teeth than adults between the ages of 20-34. This trend continued for seniors with seniors above the age of 75 having fewer teeth than those between the age of 65-74 years. It is also entirely possible that patients are more likely to seek treatment as they lose more teeth as chewing ability is greatly affected when greater number of tooth functional units are missing (Brennan et. al 2008). Loss of chewing function has been shown to negatively impact quality of life (Bortoluzzi et. al 2012), which may be a strong motivator for these patients to seek treatment as they lose teeth in the later decades of their lives.

4.2 Observance of guidelines

The objective of this part of the study was to determine if the Graduate Periodontics and Prosthodontics programs were compliant with the published and accepted guidelines with respect to CBCT prescriptions for implant treatment planning. Due to its many benefits, CBCT has become that standard of care for implant treatment planning. However, as stated in the AAOMR guidelines (Tyndall et. al 2012), CBCT should not be the initial image modality of choice for implant patients. Rather, the initial radiographic examination should employ panoramic and intraoral imaging as necessary. This is because the purpose of the initial examination is not limited to implant related treatment. Condition of the entire dentition, presence of any abnormalities and pathologies and specific characteristics of the edentulous sites all need to be identified during the initial visit (Tyndall et. al 2012). The unnecessary radiation dosage of large FOV CBCT scans cannot be justified for this purpose. Therefore, specific areas that would benefit from supplementing information through CBCT need to be identified through conventional radiography during the initial examination. Subsequently, the smallest FOV that would yield the necessary information for diagnosis and treatment planning should be selected. In the Graduate Periodontics department, 95% of the CBCT scans prescribed were preceded by a conventional two-dimensional image (Figure 24). In the Graduate Prosthodontics department, 94% of the CBCT images were accompanied by a previously taken conventional image (Figure 26). Although all CBCTs prescriptions should be made after conventional imaging has been exhausted, both programs were largely in compliance with the accepted guidelines. The CBCT referral form at UBC includes a section where the resident must select whether a conventional image is present. Furthermore, if a conventional exists, the type of image i.e. Panoramic, PA or BW found in the patient's electronic health record must be indicated on the referral form (Appendix A). This serves as a quality control step by prompting the resident to look for a conventional image in the patient's chart and review it prior to subjecting the patient to a CBCT. When reviewing the type of conventional image that was present, a vast majority of these patients had a panoramic image taken prior to CBCT in both the Graduate Periodontics and Prosthodontics departments (Figures 25 and 27). The conventional image was considered to be current if it taken within two years of the CBCT scan, regardless of the type of image. If two or more different types of images were present for the patient, as was the case for the majority, then only the most recent image was evaluated. Majority of the CBCT referrals also only referenced the newest image in that section of the form. The AAOMR recommends that Panoramic radiograph be taken for all implant patients as part of the initial examination (Tyndall et. al 2012). This was in fact the case for a large majority of the patients in both departments. However, a significant number of these panoramic radiographs were supplemented by subsequent intraoral image. As mentioned earlier, in these cases, only the most recent image was reviewed. A few patients had only a panoramic image in their chart. These were mostly patients who were completely edentulous. Panoramic radiography is in fact the imaging modality of choice for these patients and, for majority, no further intraoral imaging is required (Sumer et. al 2007). This can explain why panoramic radiographs constituted majority of pre-CBCT imaging in our audit.

In the Graduate Periodontics program, 84 patients were exposed to multiple scans. However, all 84 of these patients were identified to have a deficiency in the alveolar ridge width or height after their first exposure. Consequently, these patients had a later ridge and/or a sinus augmentation performed. The second CBCT prescription was for the purpose of evaluating the bone quantity and quality after these procedures. This falls within the recommendations of AAOMR and the AAP. Therefore, none of these patients received unnecessary radiation.

4.3 CBCT imaging parameters

Changes in imaging parameters affect both the image quality and radiation dose. For example, increase in the size of field of view, tube voltage (kVp), tube current (mA) and exposure time increase the amount of radiation received by the patient (Pauwels et. al 2015). Spatial resolution is the ability of being able to distinguish between two adjacent points or structures (Pauwels et. al 2015). In other words, spatial resolution refers to the ability of resolving fine details of structure of interest within an image (Brullmann et. al 2015). It is determined by many factors including the focal spot size, physical pixel size on the detector, reconstructed voxel size, and smoothening filters during image reconstruction (Brullmann et. al 2015, Pauwels et. al 2015). Anatomic details during implant planning can be measured more accurately when spatial resolution is high (Brullmann et. al 2015). Noise, which is random inconsistencies in the voxel values within an image, is directly related to kVp and mA (Pauwels et. al 2015). Spatial resolution and noise are related in such a way that parameters that improve one will usually degrade the other. Therefore, a balance must be achieved. It is recommended that kVp and mA levels should be selected according to the required image quality (Pauwels et. al 2015).

There was a clear trend towards high resolution images for the small FOV in the Graduate Periodontics program, especially in the last year of this audit. Although the Carestream 9300 software refers to the two available selections for the small FOV as low and high-resolution, what they reflect are the changes in imaging parameters to obtain a subjectively and objectively better-quality image. Prior to 2018, high resolution imaging for the small FOV was seldomly prescribed in the department. This shift in philosophy was due to increasing complaints in the department towards some low-resolution images being inadequate in visualizing the border of vital structures such as the inferior alveolar nerve canal. However, the higher quality images come at an increased radiation cost to the patient. Specifically, the difference in radiation exposure between the small FOV low and higher resolution images is 257 Gray. Therefore, it was important to explore whether changing the imaging parameters results in significant changes in the image quality that can be measured in an objective manner.

The main aim this part of the study was to evaluate whether altering the mA and kVp values will result in linear measurement changes on CBCT volumes. We attempted to answer this by measuring the distance between two adjacent implants placed in a model. Previous studies have revealed that there is potential for discrepancy between digital planning and clinical placement of dental implants using stereolithographic guides (Skjerven et. al 2019). Implant position can be off by as much as 2.74mm at the level of the alveolar crest and up to 5.16mm at the implant apex from where it was initially planned during digital planning (Skjerven et. al 2019). Therefore, we decided to take three measurements along the implant body to account for any deviations. Furthermore, we also subsequently placed a third implant on the opposite side to determine whether additional metal artifacts and scatter will have a significant effect on our measurements. The results of this study reveal that although changing the mA and kVp values does not affect the linear measurements between two implants in the Carestream software overall for both the small and medium FOVs, the null hypothesis can only be rejected partially. When comparing certain mA and kVp values, statistically significant difference in the mean linear distance between the two implants were noted for both the small and medium FOVs. These differences in the mean distance ranged between 0.1 and 1.1mm and were the largest when comparing the two extremes for both mA and kVp. For example, when comparing the small FOV scan taken at 2mA with one taken at 10mA, the mean difference in measurements was 1.1mm at crestal, mid and apical levels. This becomes even more evident when we consider that although the mean difference was 1.1mm, the greatest discrepancy seen in the distance measurements was 1.6mm. Not only is this statistically significant but also clinically relevant. A 1.6mm difference has the potential for significant clinical implications. Implant surgery involves precise placement and does not allow a great degree of error in the final implant position. Not only is this important from the restorative perspective but also in avoiding potential injury to vital structures. A minimum 2mm zone of safety is usually recommended to avoid any potential complications (Juodzbalys et. al 2010). This means that there should be at least 2mm between the final implant position and any adjacent vital structures. A 1.6mm error can translate into encroachment of this safety zone, which increases the risk of possible adverse outcomes. Placing the implant 1mm instead of 2mm away from the inferior alveolar nerve canal, for example, can result in compression of the bone housing and the nerve inside (Steinberg et. al 2015). This can result in substantial and lasting negative outcomes for the patient.

When comparing the differences between small and medium FOVs, no differences were noted overall. However, like the previous results, there were statistically significant differences for certain mA values. These differences can potentially be explained by the difference in voxel size between the small and medium FOVs. Carestream 9300 allows for a voxel size of 0.09mm for the small FOV and 0.18mm for the medium FOV. As mentioned previously, the voxel size is related directly to spatial resolution and therefore the ability to decipher details within structures. (Pauwels et. al 2015). The smaller voxel size for the small FOV scans signifies that the measurements points were likely better distinguished than the medium FOV scans. Although the mean difference between measurements was statistically significant, it was only 0.1mm. It is possible that this difference could be due the difference in the voxel size between the small and medium FOVs. The smaller voxels in the small FOV result in greater spatial resolution and better visualization of the implant details within the two-dimensional projections of the CBCT volume. This difference in resolution can potentially account for the small difference in mean measurement distance seen between the small and medium FOVs. Regardless, this difference is unlikely to be meaningful in clinical practice.

Presence of metal objects such as metal restorations, brackets, root filling material and dental implants lead to beam hardening and photon starvation, producing metal artifacts (MacDonald 2020, page 83). Metal artifacts increase noise and decrease contrast, which in turn can make measurements more difficult. It has been reported that metal artifacts lead to deviations in implant placement when a surgical guide designed with the help of a CBCT scan was used (Kim et. al 2019). However, the results of our study indicate that the addition of a third implant did not have any statistically significant effects on the measurements between the implants placed initially. One explanation could be that the third implant placed on the opposite side of the model, was at a position which is quite distant from the other two implants. Consequently, the scatter and metal artifacts were not significant enough to affect the measurements. Furthermore, we can attempt to extrapolate the results of this study to measurements between anatomic and biological structures when implants or metallic restoration are absent. It is reasonable to assume that when altering the mA and kVp values in the same manner as in this study in the absence of metal objects, the measurement discrepancies will not be as significant between two anatomical structures due to the lack of image deterioration by metal artifacts.

Based on the objective data collected and a subjective evaluation of the images obtained, the best images for the small FOV were obtained when the imaging parameters were in line with those recommended by the manufacturer. The most accurate measurements at the crestal level were acquired when the tube current was 5mA and tube voltage was either 80 or 90 kVp. These images also subjectively appeared to be the best in terms of visualizing the fine details within the implant bodies. Note that the manufacturers recommendation for small FOV imaging parameters are tube current of 5mA and tube voltage of 84kVp. For the medium FOV, the most accurate measurements at the crestal level and subjectively most detailed images were obtained when the tube current was 5mA and tube voltage was 90 kVp. This is slightly higher than the manufacturers tube current recommendation of 4mA. This discrepancy could be due to the differences in the composition of the model and human mandible in vivo, which become more apparent when the voxel size is larger and spatial resolution is lower, as is the case in the medium FOV.

4.4 Limitations

For the second part of the study, we compared the measured distances between two implants while varying imaging parameters. However, we were only able to measure the true distance between the implants at the level of crest, which was visible. The measurements taken at predetermined points along the body of the implant could not be compared to an established value. Although the implants were planned in the software at a distance of 5mm from each other through their entire length, it cannot be assumed that this was translated into the model. There are slight but important inaccuracies in all steps involved from planning to implant placement, including the guide fabrication itself and the armamentarium used in implant placement. It is almost certain that the implants were not placed exactly as they were planned. Therefore, sectioning of the model to obtain the true distance between implants would have improved our design.

Another limitation of this study is that there was no inter-examiner panel in our study. All measurements were conducted by a single examiner. Naturally, there is potential for human error in accurately determining the reference points from which the measurements originated and concluded. However, we only compared the differences in measurements and not the accuracy of measurements to the true value. Therefore, even though there was only a single examiner, the potential for any bias in the results is low as the any measurement error, if any, is expected to be consistent throughout the study.

There are also certain drawbacks that arise when using a model as a substitute for a human mandible. This model, like many others in the market, is composed of polyurethane material. Polyurethane has been shown to have a total attenuation coefficient that lies in between that of human soft tissue and bone (Akhlagi et. al 2015). Therefore, more X-rays can reach the implants when exposed to radiation in this model than would in an actual mandible at the same imaging parameters. Furthermore, this model lacks any soft-tissue or equivalent substitute. Although the attenuation coefficient of soft tissues is significantly lower than that of bone and polyurethane material, the lack of soft tissue, nonetheless, will have an impact on the measurements when compared to a human mandible in vivo. Presence or absence of soft tissue will affect both the energy and number of X-rays reaching the implants present in bone.

The human mandible consists of dense cortical bone shell that surrounds the porous, trabecular bone. This model is able to mimic this anatomical situation to a large extent. However, as seen in figure 7, the model has a radiopaque center surrounded by a radiolucent layer separating it from the rest of structure. This is not representative of the human mandibular anatomy. Although this difference is unlikely to have a substantial effect on the results of this experiment, it is worth noting.

4.5 Future Directions

This first part of this study focused on a retrospective review of EPR of patients who presented for implant related treatment at the University of British Columbia Faculty of Dentistry. It was found that there was a tendency towards higher resolution scans in order obtain images of a higher diagnostic quality. The second portion of this study then aimed at determining whether changes in CBCT imaging parameters will result in changes in accuracy as determined by measuring the distance between two adjacent implants on a single image viewing software. Although the results of this study are applicable to the clinical practice currently, it can also be used as a foundation for studies to be conducted in the future.

The design of this study made use of only one image viewing software for measurements. As noted earlier at high mA values, there was distinct loss of details and increase in scatter and metal artifacts. Both metal artifacts and scatter can be reduced in image viewing software during post-processing. It may be worthwhile repeating the second part of this study with different image viewing software that are commercially available.

Furthermore, this study used a model mandible for implant placement and imaging. A model is only an approximation of the actual anatomic structure. The study design can be modified for implant placement in an animal or human model *in vitro* and subsequent cross-sectional imaging. Although ceramic implants have been around since the late 1960s, recent advances in biomaterials have led to the development of zirconium dioxide ceramics implants (Cionca et. al 2017). These implant systems are gaining popularity among clinicians and have been shown to have a high survival rates in short term (Pierelli et. al 2017). Moreover, a difference in artifacts generated in CBCT images was recently demonstrated when comparing zirconium, titanium and titanium-zirconium alloy implants (Kocasarac et. al 2019). Substitution of the titanium alloy implants used in this study with ceramic implants may yield different results. This idea may be worth further exploration in a future study.

Chapter 5: Conclusions

5.1 Part 1

1. Vast majority of the CBCT referrals in the Graduate Periodontics and Prosthodontics departments were prescribed for the purposes of implant treatment planning
2. Majority of the time, a small FOV was selected in the Graduate Periodontics program whereas a medium FOV was most frequently selected in the Graduate Prosthodontics program. This likely reflects the complexity of cases presenting to the Prosthodontics department.
3. Patients in the sixth decade of their lives were most frequently prescribed a CBCT in both the Periodontics and Prosthodontics departments.
4. CBCT scans for the maxilla were taken more frequently than the mandible.

5.2 Part 2

1. The aim of the prescribed CBCT scans was justified and in line with the guidelines published by the AAOMR and the AAP.
2. 95% of the prescriptions for the purposes of implants in the Graduate Periodontics and 94% of the prescriptions in the Graduate Prosthodontics programs were accompanied by a conventional image that was taken prior to a CBCT.

5.3 Part 3

1. Manipulation of imaging parameters does affect the measurement between two adjacent implants for some mA and kVp values.
2. There are statistically significant differences in measurements between the small and medium FOVs for certain mA values.

3. The addition of a third implant does not affect the measurements between two adjacent implants on the opposite side.

Bibliography

Akhlaghi, P., Miri Hakimabad, H., & Rafat Motavalli, L. (2015). Determination of tissue equivalent materials of a physical 8-year-old phantom for use in computed tomography. *Radiation Physics and Chemistry, 112*, 169-176. doi:10.1016/j.radphyschem.2015.03.030

American Academy of Oral and Maxillofacial Radiology, Tyndall, D. A., & Brooks, S. L. (2000). Selection criteria for dental implant site imaging: A position paper of the American Academy of Oral and Maxillofacial Radiology. Oral Surgery, Oral Medicine, Oral Pathology, Oral Radiology and Endodontology, 89(5), 630-637. doi:10.1067/moe.2000.106336

Bhatt, M. (2017). Prescriptive pattern and clinical decision making in complicated endodontic cases using cone-beam computed tomography. (T). University of British Columbia. Retrieved from https://open.library.ubc.ca/collections/ubctheses/24/items/1.0357035

Bornstein, M. M., Scarfe, W. C., Vaughn, V. M., & Jacobs, R. (2014). Cone beam computed tomography in implant dentistry: A systematic review focusing on guidelines, indications, and radiation dose risks. International Journal of Oral & Maxillofacial Implants, 29(Supplement), 55-77. doi:10.11607/jomi.2014suppl.g1.4

Bortoluzzi, M., Traebert, J., Lasta, R., Da Rosa, T., Capella, D., & Presta, A. (2012). Tooth loss, chewing ability and quality of life. Contemporary Clinical Dentistry, 3(4), 393-397. doi:10.4103/0976-237X.107424

Brennan, D. S., Spencer, A. J., & Roberts-Thomson, K. F. (2008). Tooth loss, chewing ability and quality of life. Quality of Life Research, 17(2), 227-235. doi:10.1007/s11136-007-9293-2

Brown, J., Jacobs, R., Levring Jäghagen, E., Lindh, C., Baksi, G., Schulze, D., . . . Faculty of Odontology. (2014). Basic training requirements for the use of dental CBCT by dentists: A position paper prepared by the European Academy of DentoMaxilloFacial Radiology. Dento-Maxillo-Facial Radiology, 43(1), 20130291. doi:10.1259/dmfr.20130291

Brullmann, D., & Schulze, R. (2015). Spatial resolution in CBCT machines for dental/maxillofacial applications-what do we know today? Dentomaxillofacial Radiology, 44(1), 20140204. doi:10.1259/dmfr.20140204

Choi, I. G. G., Cortes, A. R. G., Arita, E. S., & Georgetti, M. A. P. (2018). Comparison of conventional imaging techniques and CBCT for periodontal evaluation: A systematic review. Imaging Science in Dentistry, 48(2), 79-86. doi:10.5624/isd.2018.48.2.79

Cionca, N., Hashim, D., & Mombelli, A. (2017). Zirconia dental implants: Where are we now, and where are we heading? Periodontology 2000, 73(1), 241-258. doi:10.1111/prd.12180

D'haese, J., Ackhurst, J., Wismeijer, D., De Bruyn, H., & Tahmaseb, A. (2017). Current state of the art of computer-guided implant surgery. Periodontology 2000, 73(1), 121-133. doi:10.1111/prd.12175

Hirschfeld, L., & Wasserman, B. (1978). Long-term survey of tooth loss in 600 treated periodontal patients. Journal of Periodontology, 49(5), 225-237.

Ho, W., Chen, W., Wu, S., & Hsu, H. (2008). Structure, mechanical properties, and grindability of dental Ti–Zr alloys. Journal of Materials Science: Materials in Medicine, 19(10), 3179-3186. doi:10.1007/s10856-008-3454-x

Horn, T., Harrysson, O., West II, H., Little, J., & Marcellin-Little, D. (2014). Development of a patient-specific bone analog for the biomechanical evaluation of custom implants. Rapid Prototyping Journal, 20(1), 41-49. doi:10.1108/RPJ-08-2012-0069

Juodzbalys, G., & Wang, H. (2010). Identification of the mandibular vital structures: Practical clinical applications of anatomy and radiological examination methods. Journal of Oral & Maxillofacial Research, 1(2), e1.

Katsumata, Akitoshi,DDS, PhD, Hirukawa, A., RT, Okumura, S., RT, Naitoh, Munetaka,DDS, PhD, Fujishita, Masami,DDS, PhD, Ariji, Eiichiro,DDS, PhD, & Langlais, Robert P.,DDS, MS. (2009). Relationship between density variability and imaging volume size in cone-beam computerized tomographic scanning of the maxillofacial region: An in vitro study. Oral Surgery, Oral Medicine, Oral Pathology, Oral Radiology and Endodontology, 107(3), 420-425. doi:10.1016/j.tripleo.2008.05.049

Kerkfeld, V., & Meyer, U. (2018). Higher resolution in cone beam computed tomography is accompanied by improved bone detection in peri-implant bone despite metal artifact presence. The International Journal of Oral and Maxillofacial Implants, 33(6), 1331-1338. doi:10.11607/jomi.6623

Kim, D. M., & Bassir, S. H. (2017). When is Cone-Beam computed tomography imaging appropriate for diagnostic inquiry in the management of inflammatory periodontitis? An American Academy of Periodontology best evidence review. Journal of Periodontology, 88(10), 978-998. doi:10.1902/jop.2017.160505

Kim, J., Park, Y., Shim, J., & Moon, H. (2019). The impact of metal artifacts within cone beam computed tomography data on the accuracy of computer-based implant surgery: An in vitro study. The International Journal of Oral and Maxillofacial Implants, 34(3), 585–594-594. doi:10.11607/jomi.7108

Lindhe, J., Lang, N. P., Berglundh, T., Giannobile, W. V., Sanz, M. (2015). Clinical periodontology and implant dentistry (Sixth ed., pp. 593-596). Ames, Iowa; Chichester, West Sussex: Wiley Blackwell. doi: 10.1002/ 9780470672488

MacDonald, D. (2020). Oral and maxillofacial radiology: A diagnostic approach (Second ed., pp 83-103). Hoboken, NJ: Wiley-Blackwell. doi: 10.1002/9781118786734

MacDonald, D. (2011). Oral and maxillofacial radiology: A diagnostic approach. (First ed., pp 59-60). Ames, Iowa; Chichester, West Sussex: Wiley-Blackwell Online Books, & Wiley Online Library. doi: 10.1002/9781119218739

Mallya, S. M., & Lam, E. W. N. (2019). White and Pharoah's oral radiology: Principles and interpretation (8th ed.). St. Louis, Missouri: Elsevier. ISBN: 9780323543835

Mandelaris, G. A., Scheyer, E. T., Evans, M., Kim, D., McAllister, B., Nevins, M. L., Sarment, D. (2017). American Academy of Periodontology Best Evidence Consensus Statement on Selected Oral Applications for Cone-Beam computed tomography. Journal of Periodontology, 88(10), 939-945. doi:10.1902/jop.2017.170234

Misch, K. A., Yi, E. S., & Sarment, D. P. (2006). Accuracy of cone beam computed tomography for periodontal defect measurements. Journal of Periodontology, 77(7), 1261-1266. doi:10.1902/jop.2006.050367

Neto, R., Hiramatsu, D., Suedam, V., Conti, P., & Rubo, J. (2011). Validation of an experimental polyurethane model for biomechanical studies on implant-supported prosthesis - compression tests. Journal of Applied Oral Science, 19(1), 47-51. doi:10.1590/S1678-77572011000100010

Patel, S., Durack, C., Abella, F., Shemesh, H., Roig, M., & Lemberg, K. (2015). Cone beam computed tomography in endodontics - a review. International Endodontic Journal, 48(1), 3-15. doi:10.1111/iej.12270

Pauwels, R., Araki, K., Siewerdsen, J. H., & Thongvigitmanee, S. S. (2015). Technical aspects of dental CBCT: State of the art. Dentomaxillofacial Radiology, 44(1), 20140224. doi:10.1259/dmfr.20140224

Pieralli, S., Kohal, R. J., Jung, R. E., Vach, K., & Spies, B. C. (2017). Clinical outcomes of zirconia dental implants: A systematic review. Los Angeles, CA: SAGE Publications. doi:10.1177/0022034516664043

Renton, T., Dawood, A., Shah, A., Searson, L., & Yilmaz, Z. (2012). Post-implant neuropathy of the trigeminal nerve. A case series. British Dental Journal, 212(11), E17. doi:10.1038/sj.bdj.2012.497

Russell, S. L., Gordon, S., Lukacs, J. R., & Kaste, L. M. (2013). Sex/gender differences in tooth loss and edentulism: Historical perspectives, biological factors, and sociologic reasons. The Dental Clinics of North America, 57(2), 317-337. doi: 10.1016/j.cden.2013.02.006

Schoenbaum, T. R. (2018). Implants in the aesthetic zone: A guide for treatment of the partially edentulous patient. CH: Springer.

Schwarz, M. S., Rothman, S. L., Rhodes, M. L., & Chafetz, N. (1987). Computed tomography: Part I. preoperative assessment of the mandible for endosseous implant surgery. The International Journal of Oral and Maxillofacial Implants, 2(3), 137.

Skjerven, H., Riis, U. H., Herlofsson, B. B., & Ellingsen, J. E. (2019). In vivo accuracy of implant placement using a full digital planning modality and stereolithographic guides. The International Journal of Oral and Maxillofacial Implants, 34(1), 124-132. doi:10.11607/jomi.6939

Steinberg, M. J., & Kelly, P. D. (2015). Implant-related nerve injuries. Dental Clinics of North America, 59(2), 357-373. doi:10.1016/j.cden.2014.10.003

Sumer, A. P., Sumer, M., Guler, A. U., & Bicer, I. (2007). Panoramic radiographic examination of edentulous mouths. Quintessence International, 38(7), E399-E403.

The American Dental Association Council on Scientific Affairs, Amer Dental Assoc Council Sci, & American Dental Association Council on Scientific Affairs. (2012). The use of cone-beam computed tomography in dentistry an advisory statement from the American Dental Association Council on Scientific Affairs. The Journal of the American Dental Association, 143(8), 899-902. doi:10.14219/jada.archive.2012.0295

Upadhyaya, C., & Humagain, M. (2009). The pattern of tooth loss due to dental caries and periodontal disease among patients attending dental department (OPD), Dhulikhel Hospital, Kathmandu University Teaching Hospital (KUTH), Nepal. Kathmandu University Medical Journal, 7(25), 59.

Vandenberghe, B., Jacobs, R., & Yang, J. (2008). Detection of periodontal bone loss using digital intraoral and cone beam computed tomography images: An in vitro assessment of bony and/or infrabony defects. Dentomaxillofacial Radiology, 37(5), 252-260. doi:10.1259/dmfr/57711133

Vijay, G., & Raghavan, V. (2013). Radiology in periodontics. Journal of Indian Academy of Oral Medicine and Radiology, 25(1), 24-29. doi:10.5005/jp-journals-10011-1334

Watanabe, H., Honda, E., Tetsumura, A., & Kurabayashi, T. (2011). A comparative study for spatial resolution and subjective image characteristics of a multi-slice CT and a cone-beam CT for dental use. European Journal of Radiology, 77(3), 397-402. doi:10.1016/j.ejrad.2009.09.023

Younes, F., Cosyn, J., De Bruyckere, T., Cleymaet, R., Bouckaert, E., & Eghbali, A. (2018). A randomized controlled study on the accuracy of free-handed, pilot-drill guided and fully guided implant surgery in partially edentulous patients. Journal of Clinical Periodontology, 45(6), 721-732. doi:10.1111/jcpe.12897

Appendices

Appendix A

○ DMD Comprehensive Care	○ DMD Urgent Care	○ Faculty Practise	○ Grad Endo	○ Grad Ortho
○ Grad Pediatrics	○ Grad Perio	○ Grad Prosth	○ OHC-Oral Surgery	○ Oral Medicine
○ Pharmacists Clinic	- --	◉ Cone Beam CT	○ DMD Implant	○ Geriatric Dentistry
○ Staff RDH from DMD	○ Staff RDH from Grad Perio	- --	- --	- --

Special Instructions For Cone Beam CT Referrals:

Prior to initiating a referral, DMD students:

- should provide clinical reasons including details of significant features (see the 5s and 3 Ds in Chapter 1 in MacDonald's Oral and maxillofacial radiology: a diagnostic approach. Wiley 2011). A differential diagnosis must be included, ranking the most likely and/or clinically most significant lesion at the top. (see Table 1.1 in MacDonald's Oral and maxillofacial radiology: a diagnostic approach. Wiley 2011).
- ensure that all appropriate clinical and conventional radiological investigations have been prescribed, performed, recorded and reported.
- if having ascertained from the patient a prior history of surgery or treatment for a lesion/s in the area of interest then all records and images pertaining to this/these should be reviewed. If the treatment of this/these lesions had been provided at UBC Dentistry prior to "going digital" then previous scanned notes and analog images should be retrieved and reviewed.
- discuss with a consultant in OMFR or with Dr. David MacDonald, in the first instance.

NOTE: Approval is required either from Dr. MacDonald OR from an already credentialed/ qualified specialist in the appropriate specialty. Graduate students in any specialty, in their role as DMD intructors, CANNOT give approval as they are NOT credentialed/qualified specialists. ALL DMD referrals MUST be taken by Jodi Ekk and Sabina Reitzik.

REFERRAL FOR:

________________ (Enter Chart Number)

REQUEST FROM:

________________ (Enter Provider ID)

Indication / Reason for CBCT Investigation:
(You may select more than one Indication / Reason)

☐ Impaction	☐ Orthodontics	☐ Prosthesis ONLY scan
☐ Pathology	☐ Sinus / Airway	☐ Patient scan PLUS Prosthesis scan
☐ Endodontics	☐ Implant(s)	☐ Surgical Guide

Field of View (FOV):
(You may NOT select more than one scan site. A separate referral must be completed for EACH scan)

○ Single Site (4x4)	○ Single Site (6x6)
○ Single Jaw (10x5) Maxilla	○ Single Jaw (10x5) Mandible
○ Both Jaws (8x8)	○ Both Jaws (10x10)
○ Single Jaw (14x5)	○ Single Jaw (17x5)
○ Both Jaws (14x10)	○ Both Jaws (17x12)

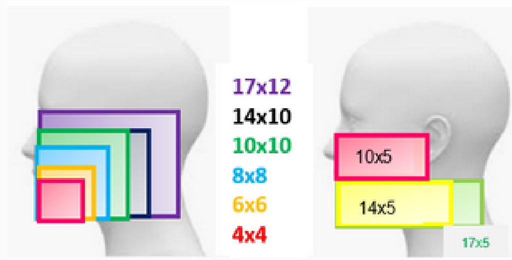

Resolution:

○ LOW resolution 125-250 µm (micrometer) voxel size ○ HIGH resolution 80 µm (micrometer) voxel size

Region of Interest (ROI) / Special Instructions
(it is necessary to provide clear Instructions to the radiographer - describe the areas of interest that must be included in the scan for it to meet your needs)
Examples:

- *both teeth proximal to 1.6 implant site and inferior half (approx.) of maxillary sinus AND if possible without sacrificing view of sinus, to also include occlusal third (approx.) of opposing arch.*
- *both teeth proximal to 4.6 implant site and inferior border of mandible AND if possible, to also include occlusal third (approx.) of opposing arch.*
- *In impacted teeth or pathology~ need to describe the area so that the radiographer can localize the area of interest in the FOV eg. anterior-posterior 11 - 25 area and laterally to include buccal plate and lingual/palatal expansion.*

Reference Images:

(include (reference to) any additional images that are available to assist with localization of the area.)

○ None available ○ Panoramic ____ (dd/mm/yyyy) ○ Other ____ (dd/mm/yyyy)

Relevant Medical History and Special Considerations

(Please identify any mobility, behavioral, or postural issues which may impact patient positioning).

Appendix B

Sample Images

<u>Small FOV</u>

mA	kVp	DAP
2	90	285

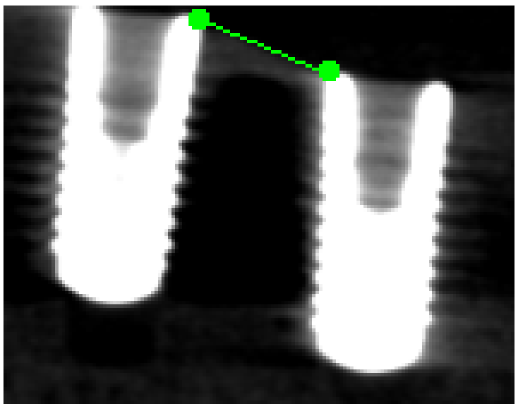

mA	kVp	DAP
5	90	713

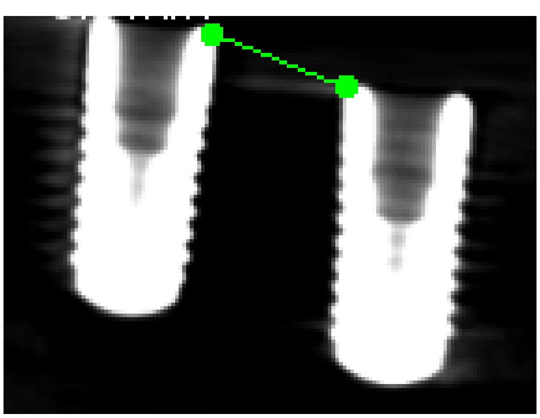

mA	kVp	DAP
10	90	1426

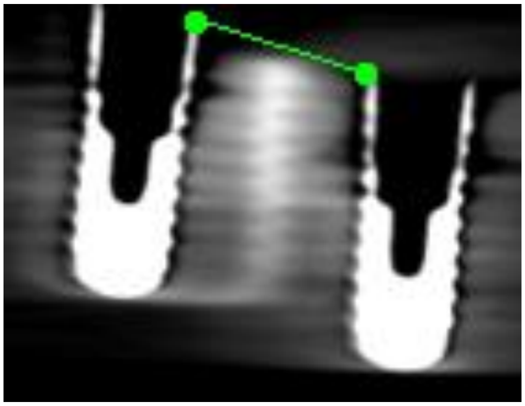

mA	kVp	DAP
5	60	215

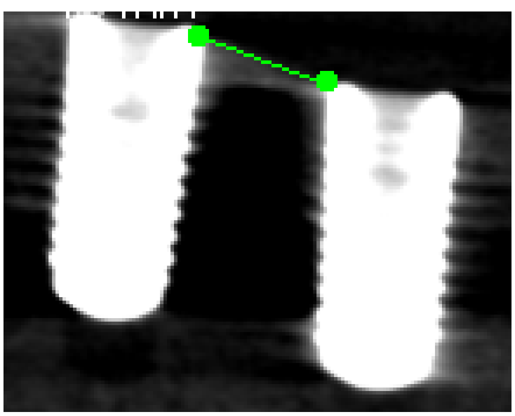

mA	kVp	DAP
5	80	523

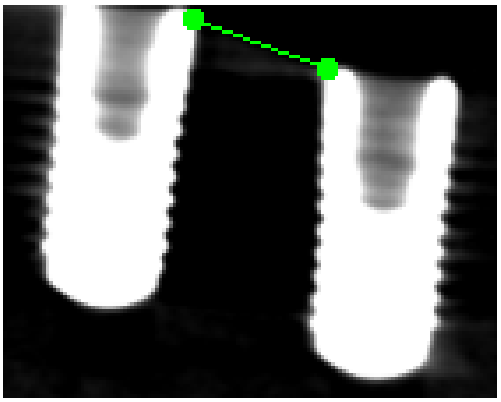

Medium FOV

mA	kVp	DAP
2	90	194

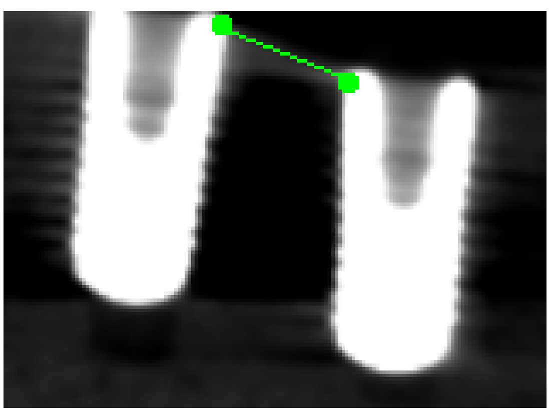

mA	kVp	DAP
4	90	388

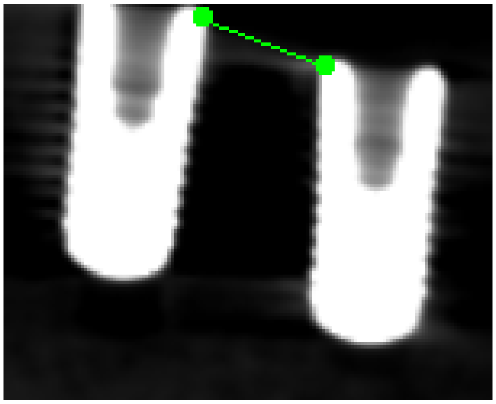

mA	kVp	DAP
5	90	486

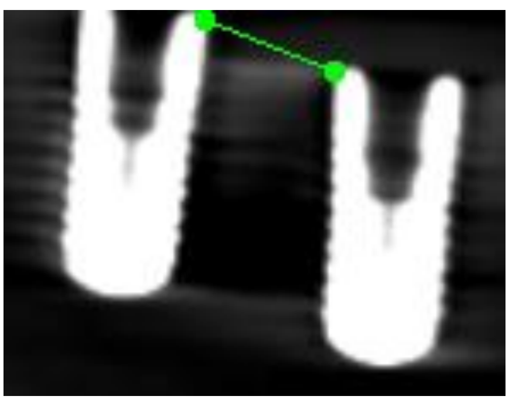

mA	kVp	DAP
10	90	971

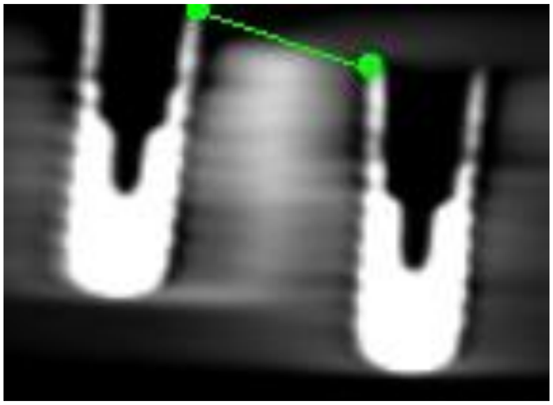

mA	kVp	DAP
4	60	115

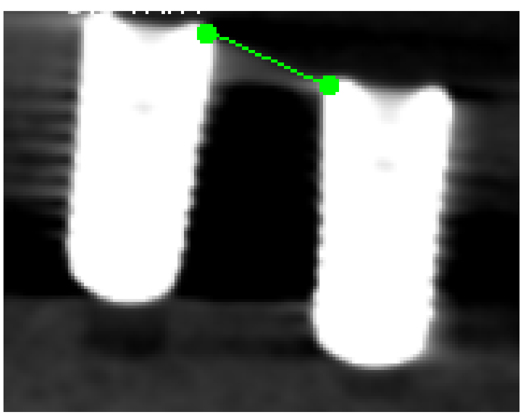

mA	kVp	DAP
4	80	285

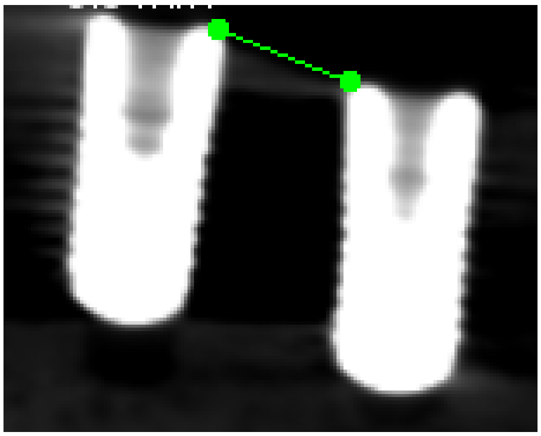

Appendix C

Data Tables – Measurements between implants

Table 1 represents results from small FOV scans with 2 implants where tube voltage (kVp) was held constant at 90kVp and tube current (mA) was varied from 2mA to 10mA in increments allowed by the Carestream software. Crest signifies measurements taken at the level of implant crest or collar. Mid represents measurements taken at the level of threads immediately adjacent to where internal screw channel terminates. Apical represents measurements taken at level of the second to last implant threads. The “S” and “A” stand for sagittal and axial planes. As mentioned earlier measurements were taken for two separate models described as “Model 1” and “Model 2.”

					Crest (S)		Mid (S)		Apical (S)		Crest (A)		Mid (A)		Apical (A)	
FOV	**kVp**	**mA**	**Scan time**	**Dose**	**Model 1**	**Model 2**	**Model 1**	**Model 2**	**Model 1**	**Model 2**	**Model 1**	**Model 2**	**Model 1**	**Model 2**	**Model 1**	**Model 2**
5x5	90	2	19.96	285	4.8	4.7	5.0	5.1	5.3	5.4	4.8	4.6	5.0	5.2	5.3	5.4
5x5	90	2.5	19.96	356	4.8	4.7	5.0	5.2	5.2	5.4	4.8	4.7	5.0	5.3	5.2	5.4
5x5	90	3.2	19.96	456	4.8	4.7	5.0	5.1	5.2	5.4	4.7	4.7	5.0	5.2	5.3	5.5
5x5	90	4	19.96	570	4.8	4.7	5.0	5.1	5.2	5.4	4.8	4.7	5.0	5.2	5.2	5.4
5x5	90	5	19.96	713	5.0	4.9	5.1	5.2	5.3	5.5	4.9	4.8	5.2	5.3	5.4	5.5
5x5	90	6.3	19.96	898	5.1	5.1	5.4	5.6	5.5	5.8	5.2	5.0	5.4	5.5	5.6	5.8
5x5	90	8	19.96	1140	5.5	5.5	5.6	5.9	5.8	6.1	5.5	5.3	5.7	5.9	5.9	6.1
5x5	90	10	19.96	1426	5.9	5.8	6.1	6.2	6.2	6.5	5.9	5.7	6.1	6.2	6.3	6.5

Table 1: Small field of view measurements with two implants and varying mA

Table 2 represents results from small field of view scans with 2 implants where mA was held constant at 5mA and kVp was varied from 60kVp to 90kVp in increments of 10.

					Crest (S)		Mid (S)		Apical (S)		Crest (A)		Mid (A)		Apical (A)	
FOV	**kVp**	**mA**	**Scan time**	**Dose**	**Model 1**	**Model 2**	**Model 1**	**Model 2**	**Model 1**	**Model 2**	**Model 1**	**Model 2**	**Model 1**	**Model 2**	**Model 1**	**Model 2**
5x5	60	5	19.96	215	4.6	4.6	4.8	5.1	5.2	5.3	4.5	4.5	4.9	5.0	5.2	5.3
5x5	70	5	19.96	356	4.8	4.7	5.0	5.2	5.2	5.4	4.8	4.6	5.0	5.2	5.2	5.4
5x5	80	5	19.96	523	4.8	4.7	5.0	5.2	5.2	5.4	4.8	4.6	5.0	5.2	5.3	5.4
5x5	90	5	19.96	713	5.0	4.9	5.1	5.2	5.3	5.5	4.9	4.8	5.2	5.3	5.4	5.5

Table 2: Small field of view measurements with two implants and varying kVp

Table 3 represents results from medium field of view scans with 2 implants where kVp was held constant at 90kVp and the mA was varied from 2mA to 10mA in increments allowed by the Carestream software.

					Crest (S)		Mid (S)		Apical (S)		Crest (A)		Mid (A)		Apical (A)	
FOV	**kVp**	**mA**	**Scan time**	**Dose**	**Model 1**	**Model 2**	**Model 1**	**Model 2**	**Model 1**	**Model 2**	**Model 1**	**Model 2**	**Model 1**	**Model 2**	**Model 1**	**Model 2**
10x5	90	2	8.01	194	4.6	4.7	5.0	5.1	5.1	5.4	4.6	4.6	5.0	5.2	5.2	5.4
10x5	90	2.5	8.01	243	4.7	4.7	4.9	5.2	5.2	5.4	4.6	4.7	5.0	5.3	5.2	5.4
10x5	90	3.2	8.01	311	4.6	4.7	5.0	5.1	5.2	5.4	4.5	4.7	5.0	5.2	5.1	5.5
10x5	90	4	8.01	388	4.8	4.7	5.1	5.1	5.3	5.4	4.8	4.7	5.0	5.2	5.3	5.4
10x5	90	5	8.01	486	5.0	4.9	5.2	5.2	5.4	5.5	4.9	4.8	5.2	5.3	5.4	5.5
10x5	90	6.3	8.01	612	5.3	5.1	5.5	5.6	5.6	5.8	5.3	5.0	5.5	5.5	5.7	5.8
10x5	90	8	8.01	777	5.6	5.5	5.8	5.9	6.0	6.1	5.6	5.3	5.8	5.9	6.1	6.1
10X5	90	10	8.01	971	5.8	5.8	6.4	6.2	6.7	6.5	5.8	5.7	6.5	6.2	6.8	6.5

Table 3: Medium field of view measurements with two implants and varying mA

Table 4 represents results from medium field of view scans with 2 implants where mA was held constant at 5mA and kVp was varied from 60kVp to 90kVp in increments of 10.

					Crest (S)		Mid (S)		Apical (S)		Crest (A)		Mid (A)		Apical (A)	
FOV	**kVp**	**mA**	**Scan time**	**Dose**	**Model 1**	**Model 2**	**Model 1**	**Model 2**	**Model 1**	**Model 2**	**Model 1**	**Model 2**	**Model 1**	**Model 2**	**Model 1**	**Model 2**
10x5	60	4	8.01	115	4.5	4.5	4.9	5.1	5.2	5.3	4.4	4.5	4.8	5.2	5.2	5.2
10x5	70	4	8.01	194	4.6	4.5	4.9	5.1	5.1	5.3	4.6	4.5	4.9	5.1	5.2	5.1
10x5	80	4	8.01	285	4.7	4.6	5.0	5.2	5.1	5.4	4.6	4.6	5.0	5.1	5.1	5.1
10x5	90	4	8.01	388	4.8	4.7	5.1	5.1	5.3	5.4	4.8	4.7	5.0	5.2	5.3	5.4

Table 4: Medium field of view measurements with two implants and varying kVp

Table 5 represents results from small field of view scans with 3 implants where kVp was held constant at 90kVp and mA was varied from 2mA to 10mA in increments allowed by the Carestream software.

					Crest (S)		Mid (S)		Apical (S)		Crest (A)		Mid (A)		Apical (A)	
FOV	**kVp**	**mA**	**Scan time**	**Dose**	**Model 1**	**Model 2**	**Model 1**	**Model 2**	**Model 1**	**Model 2**	**Model 1**	**Model 2**	**Model 1**	**Model 2**	**Model 1**	**Model 2**
5x5	90	2	19.96	285	4.7	4.6	5.0	5.2	5.2	5.4	4.8	4.7	5.0	5.2	5.1	5.4
5x5	90	2.5	19.96	356	4.8	4.7	5.0	5.2	5.2	5.4	4.7	4.6	5.1	5.2	5.2	5.4
5x5	90	3.2	19.96	456	4.8	4.7	5.0	5.2	5.2	5.5	4.8	4.6	5.0	5.2	5.2	5.4
5x5	90	4	19.96	570	4.8	4.8	5.0	5.2	5.2	5.4	4.8	4.7	5.0	5.2	5.2	5.5
5x5	90	5	19.96	713	4.9	4.9	5.1	5.3	5.2	5.5	4.9	4.9	5.1	5.3	5.3	5.5
5x5	90	6.3	19.96	898	5.2	5.1	5.4	5.5	5.5	5.8	5.1	5.0	5.4	5.6	5.6	5.8
5x5	90	8	19.96	1140	5.5	5.4	5.6	5.8	5.8	6.1	5.4	5.3	5.6	5.8	5.8	6.1
5x5	90	10	19.96	1426	5.8	5.6	6	6.2	6.1	6.5	5.8	5.6	6	6.3	6.2	6.5

Table 5: Small field of view measurements with 3 implants and varying mA

Table 6 represents results from small field of view scans with 3 implants where mA was held constant at 5mA and kVp was varied from 60kVp to 90kVp in increments of 10.

					Crest (S)		Mid (S)		Apical (S)		Crest (A)		Mid (A)		Apical (A)	
FOV	**kVp**	**mA**	**Scan time**	**Dose**	**Model 1**	**Model 2**	**Model 1**	**Model 2**	**Model 1**	**Model 2**	**Model 1**	**Model 2**	**Model 1**	**Model 2**	**Model 1**	**Model 2**
5x5	60	5	19.96	215	4.7	4.6	4.9	5.1	5.2	5.3	4.6	4.5	4.9	5.1	5.1	5.3
5x5	70	5	19.96	356	4.8	4.7	5.0	5.2	5.2	5.4	4.7	4.7	5.0	5.2	5.2	5.4
5x5	80	5	19.96	523	4.9	4.8	5.0	5.2	5.2	5.4	4.9	4.8	5.0	5.2	5.2	5.4
5x5	90	5	19.96	713	4.9	4.9	5.1	5.3	5.2	5.5	4.9	4.9	5.1	5.3	5.3	5.5

Table 6: Small field of view measurements with 3 implants and varying kVp

Table 7 represents results from medium field of view scans with 3 implants where kVp was held constant at 90kVp and mA was varied from 2mA to 10mA in increments allowed by the Carestream software.

					Crest (S)		Mid (S)		Apical (S)		Crest (A)		Mid (A)		Apical (A)	
FOV	**kVp**	**mA**	**Scan time**	**Dose**	**Model 1**	**Model 2**	**Model 1**	**Model 2**	**Model 1**	**Model 2**	**Model 1**	**Model 2**	**Model 1**	**Model 2**	**Model 1**	**Model 2**
10x5	90	2	8.01	194	4.6	4.6	4.9	5.1	5.1	5.3	4.5	4.6	4.8	5.0	5.1	5.3
10x5	90	2.5	8.01	243	4.7	4.6	5.0	5.1	5.2	5.4	4.7	4.7	5.0	5.1	5.2	5.4
10x5	90	3.2	8.01	311	4.7	4.7	5.0	5.2	5.2	5.4	4.8	4.7	5.0	5.1	5.2	5.4
10x5	90	4	8.01	388	4.8	4.8	5.1	5.2	5.3	5.4	4.7	4.7	5.1	5.2	5.2	5.4
10x5	90	5	8.01	486	5.0	5.0	5.2	5.3	5.4	5.6	5.0	4.9	5.2	5.3	5.4	5.6
10x5	90	6.3	8.01	612	5.3	5.2	5.5	5.5	5.7	5.7	5.3	5.2	5.4	5.6	5.7	5.8
10x5	90	8	8.01	777	5.7	5.8	5.8	6.0	6.0	6.3	5.5	5.7	5.8	6.1	6.0	6.4
10x5	90	10	8.01	971	5.7	6.0	6.4	6.5	6.5	6.8	5.7	6.1	6.4	6.5	6.5	6.8

Table 7: Medium field of view measurements with 3 implants and varying mA

Table 8 represents results from medium field of view scans with 3 implants where mA was held constant at 5mA and kVp was varied from 60kVp to 90kVp in increments of 10.

					Crest (S)		Mid (S)		Apical (S)		Crest (A)		Mid (A)		Apical (A)	
FOV	**kVp**	**mA**	**Scan time**	**Dose**	**Model 1**	**Model 2**	**Model 1**	**Model 2**	**Model 1**	**Model 2**	**Model 1**	**Model 2**	**Model 1**	**Model 2**	**Model 1**	**Model 2**
10x5	60	4	8.01	115	4.5	4.5	4.8	5.0	5.1	5.2	4.5	4.5	4.8	5.0	5.1	5.2
10x5	70	4	8.01	194	4.6	4.6	4.8	5.1	5.2	5.3	4.5	4.7	4.8	5.0	5.2	5.3
10x5	80	4	8.01	285	4.7	4.7	5.0	5.1	5.3	5.3	4.7	4.7	5.0	5.1	5.3	5.3
10x5	90	4	8.01	388	4.8	4.8	5.1	5.2	5.3	5.4	4.7	4.7	5.1	5.2	5.2	5.4

Table 8: Medium field of view measurements with 3 implants and varying kVp

Appendix D

Tables from Statistical Analysis

Table Analyzed	5x5 90KV - 2 implants				
Two-way RM ANOVA	Matching: Both factors				
Assume sphericity?	No				
Alpha	0.05				
Source of Variation	**% of total variation**	**P value**	**P value summary**	**Significant?**	**Geisser-Greenhouse's epsilon**
mA	69.19	0.0268	*	Yes	0.1429
Distance	26.75	0.1837	ns	No	0.2000
mA x Distance	0.3470	0.4561	ns	No	1.000
Subject x mA	0.1231				
Subject x Distance	2.357				
Subject	0.8960				
ANOVA table	**SS**	**DF**	**MS**	**F (DFn, DFd)**	**P value**
mA	13.52	7	1.932	F (1.000, 1.000) = 561.9	P=0.0268
Distance	5.228	5	1.046	F (1.000, 1.000) = 11.35	P=0.1837
mA x Distance	0.06781	35	0.001938	F (35.00, 35.00) = 1.038	P=0.4561
Subject x mA	0.02406	7	0.003438		
Subject x Distance	0.4605	5	0.09210		
Subject	0.1751	1	0.1751		
Residual	0.06531	35	0.001866		

Table 1: mA vs distance for small field of view statistical analysis

Table Analyzed	10x5 90KV - 2 implants				
Two-way RM ANOVA	Matching: Both factors				
Assume sphericity?	No				
Alpha	0.05				
Source of Variation	**% of total variation**	**P value**	**P value summary**	**Significant?**	**Geisser-Greenhouse's epsilon**
mA	69.68	0.0856	ns	No	0.1429
Distance	26.59	0.0860	ns	No	0.2000
mA x Distance	0.8270	0.6260	ns	No	1.000
Subject x mA	1.275				
Subject x Distance	0.4916				
Subject	0.2180				
ANOVA table	**SS**	**DF**	**MS**	**F (DFn, DFd)**	**P value**
mA	17.61	7	2.516	F (1.000, 1.000) = 54.63	P=0.0856
Distance	6.722	5	1.344	F (1.000, 1.000) = 54.09	P=0.0860
mA x Distance	0.2091	35	0.005973	F (35.00, 35.00) = 0.8964	P=0.6260
Subject x mA	0.3224	7	0.04606		
Subject x Distance	0.1243	5	0.02485		
Subject	0.05510	1	0.05510		
Residual	0.2332	35	0.006664		
Data summary					
Number of columns (Distance)	6				
Number of rows (mA)	8				
Number of subjects (Subject)	2				
Number of missing values	0				

Table 2: mA vs distance for medium field of view statistical analysis

Table Analyzed	5mA variable KV (5x5) - 2 implants				
Two-way RM ANOVA	Matching: Both factors				
Assume sphericity?	No				
Alpha	0.05				
Source of Variation	**% of total variation**	**P value**	**P value summary**	**Significant?**	**Geisser-Greenhouse's epsilon**
kVp	10.84	0.0647	ns	No	0.3333
Distance	79.73	0.1592	ns	No	0.2000
kVp x Distance	1.329	0.4499	ns	No	0.06667
Subject x kVp	0.1126				
Subject x Distance	5.204				
Subject	1.825				
ANOVA table	**SS**	**DF**	**MS**	**F (DFn, DFd)**	**P value**
kVp	0.4008	3	0.1336	F (1.000, 1.000) = 96.20	P=0.0647
Distance	2.949	5	0.5898	F (1.000, 1.000) = 15.32	P=0.1592
kVp x Distance	0.04917	15	0.003278	F (1.000, 1.000) = 1.372	P=0.4499
Subject x kVp	0.004167	3	0.001389		
Subject x Distance	0.1925	5	0.03850		
Subject	0.06750	1	0.06750		
Residual	0.03583	15	0.002389		
Data summary					
Number of columns (Distance)	6				
Number of rows (kVp)	4				
Number of subjects (Subject)	2				
Number of missing values	0				

Table 3: Statistical analysis for kVp vs measured distance for small field of view

Table Analyzed	4mA variable KV (10x5) - 2 implants				
Two-way RM ANOVA	Matching: Both factors				
Assume sphericity?	No				
Alpha	0.05				
Source of Variation	**% of total variation**	**P value**	**P value summary**	**Significant?**	**Geisser-Greenhouse's epsilon**
kVp	5.323	0.1782	ns	No	0.3333
Distance	85.04	0.1332	ns	No	0.2000
kVp x Distance	2.096	0.4544	ns	No	0.06667
Subject x kVp	0.4401				
Subject x Distance	3.835				
Subject	1.697				
ANOVA table	**SS**	**DF**	**MS**	**F (DFn, DFd)**	**P value**
kVp	0.2117	3	0.07056	F (1.000, 1.000) = 12.10	P=0.1782
Distance	3.382	5	0.6763	F (1.000, 1.000) = 22.17	P=0.1332
kVp x Distance	0.08333	15	0.005556	F (1.000, 1.000) = 1.333	P=0.4544
Subject x kVp	0.01750	3	0.005833		
Subject x Distance	0.1525	5	0.03050		
Subject	0.06750	1	0.06750		
Residual	0.06250	15	0.004167		
Data summary					
Number of columns (Distance)	6				
Number of rows (kVp)	4				
Number of subjects (Subject)	2				
Number of missing values	0				

Table 4: Statistical analysis for kVp vs measured distance for medium field of view

Table Analyzed	2 impl 90KV 5x5 vs 10x5				
Two-way RM ANOVA	Matching: Both factors				
Assume sphericity?	No				
Alpha	0.05				
Source of Variation	**% of total variation**	**P value**	**P value summary**	**Significant?**	**Geisser-Greenhouse's epsilon**
mA	69.07	0.0484	*	Yes	0.1429
Distance	26.69	0.1404	ns	No	0.09091
mA x Distance	0.9887	0.5076	ns	No	0.01299
Subject x mA	0.4014				
Subject x Distance	1.342				
Subject	0.4758				
ANOVA table	**SS**	**DF**	**MS**	**F (DFn, DFd)**	**P value**
mA	30.97	7	4.424	F (1.000, 1.000) = 172.1	P=0.0484
Distance	11.97	11	1.088	F (1.000, 1.000) = 19.89	P=0.1404
mA x Distance	0.4433	77	0.005758	F (1.000, 1.000) = 0.9534	P=0.5076
Subject x mA	0.1800	7	0.02571		
Subject x Distance	0.6017	11	0.05470		
Subject	0.2133	1	0.2133		
Residual	0.4650	77	0.006039		
Data summary					
Number of columns (Distance)	12				
Number of rows (mA)	8				
Number of subjects (Subject)	2				
Number of missing values	0				

Table 5: Statistical analysis for comparison between small and medium fields of view for varying mA values

Table Analyzed	5x5 vs 10x5 kV (Model 1 and 2) - 2implants				
Two-way ANOVA	Ordinary				
Alpha	0.05				
Source of Variation	**% of total variation**	**P value**	**P value summary**	**Significant?**	
Interaction	1.898	0.4072	ns	No	
kVp	7.215	<0.0001	****	Yes	
Distance	82.30	<0.0001	****	Yes	
ANOVA table	**SS**	**DF**	**MS**	**F (DFn, DFd)**	**P value**
Interaction	0.1492	15	0.009944	F (15, 72) = 1.061	P=0.4072
kVp	0.5671	3	0.1890	F (3, 72) = 20.16	P<0.0001
Distance	6.468	5	1.294	F (5, 72) = 138.0	P<0.0001
Residual	0.6750	72	0.009375		
Data summary					
Number of columns (Distance)	6				
Number of rows (kVp)	4				
Number of values	96				

Table 6: Statistical analysis for comparison between small and medium field of views for varying kVp values

Table Analyzed	5x5 90KV - 2 vs 3 implants				
Two-way RM ANOVA	Matching: Both factors				
Assume sphericity?	No				
Alpha	0.05				
Source of Variation	**% of total variation**	**P value**	**P value summary**	**Significant?**	**Geisser-Greenhouse's epsilon**
mA	67.08	0.0130	*	Yes	0.1429
Distance	27.82	0.1960	ns	No	0.09091
mA x Distance	0.5458	0.4479	ns	No	0.01299
Subject x mA	0.02795				
Subject x Distance	2.814				
Subject	1.316				
ANOVA table	**SS**	**DF**	**MS**	**F (DFn, DFd)**	**P value**
mA	25.50	7	3.643	F (1.000, 1.000) = 2400	P=0.0130
Distance	10.58	11	0.9615	F (1.000, 1.000) = 9.887	P=0.1960
mA x Distance	0.2075	77	0.002695	F (1.000, 1.000) = 1.389	P=0.4479
Subject x mA	0.01063	7	0.001518		
Subject x Distance	1.070	11	0.09725		
Subject	0.5002	1	0.5002		
Residual	0.1494	77	0.001940		
Data summary					
Number of columns (Distance)	12				
Number of rows (mA)	8				
Number of subjects (Subject)	2				
Number of missing values	0				

Table 7: Statistical analysis for 2 vs 3 implants for small field of view with varying mA

Table Analyzed	5mA variable KV (5x5) - 2 and 3 implants				
Two-way RM ANOVA	Matching: Both factors				
Assume sphericity?	No				
Alpha	0.05				
Source of Variation	**% of total variation**	**P value**	**P value summary**	**Significant?**	**Geisser-Greenhouse's epsilon**
KV	10.20	0.0260	*	Yes	0.3333
Distance	78.29	0.1683	ns	No	0.09091
KV x Distance	1.762	0.3877	ns	No	0.03030
Subject x KV	0.01705				
Subject x Distance	5.734				
Subject	3.139				
ANOVA table	**SS**	**DF**	**MS**	**F (DFn, DFd)**	**P value**
KV	0.6853	3	0.2284	F (1.000, 1.000) = 598.1	P=0.0260
Distance	5.261	11	0.4783	F (1.000, 1.000) = 13.65	P=0.1683
KV x Distance	0.1184	33	0.003589	F (1.000, 1.000) = 2.056	P=0.3877
Subject x KV	0.001146	3	0.0003819		
Subject x Distance	0.3853	11	0.03503		
Subject	0.2109	1	0.2109		
Residual	0.05760	33	0.001746		
Data summary					
Number of columns (Distance	12				
Number of rows (KV)	4				
Number of subjects (Subject)	2				
Number of missing values	0				

Table 8: Statistical analysis for 2 vs 3 implants for small field of view with varying kVp

Table Analyzed	10x5 90KV - 2 vs 3 implants				
Two-way RM ANOVA	Matching: Both factors				
Assume sphericity?	No				
Alpha	0.05				
Source of Variation	**% of total variation**	**P value**	**P value summary**	**Significant?**	**Geisser-Greenhouse's epsilon**
mA	72.95	0.0376	*	Yes	0.1429
Distance	23.04	0.1017	ns	No	0.09091
mA x Distance	1.180	0.5133	ns	No	0.01299
Subject x mA	0.2557				
Subject x Distance	0.5987				
Subject	0.6876				
ANOVA table	**SS**	**DF**	**MS**	**F (DFn, DFd)**	**P value**
mA	38.99	7	5.571	F (1.000, 1.000) = 285.3	P=0.0376
Distance	12.32	11	1.120	F (1.000, 1.000) = 38.48	P=0.1017
mA x Distance	0.6308	77	0.008193	F (1.000, 1.000) = 0.9198	P=0.5133
Subject x mA	0.1367	7	0.01952		
Subject x Distance	0.3200	11	0.02909		
Subject	0.3675	1	0.3675		
Residual	0.6858	77	0.008907		
Data summary					
Number of columns (Distance)	12				
Number of rows (mA)	8				
Number of subjects (Subject)	2				
Number of missing values	0				

Table 9: Statistical analysis for 2 vs 3 implants for medium field of view with varying mA

Table Analyzed	4mA variable KV (10x5) - 2 and 3 implants				
Two-way RM ANOVA	Matching: Both factors				
Assume sphericity?	No				
Alpha	0.05				
Source of Variation	**% of total variation**	**P value**	**P value summary**	**Significant?**	**Geisser-Greenhouse's epsilo**
Kv	6.567	0.0411	*	Yes	0.3333
Distance	81.95	0.1509	ns	No	0.09091
Kv x Distance	2.412	0.4077	ns	No	0.03030
Subject x Kv	0.02739				
Subject x Distance	4.779				
Subject	2.920				
ANOVA table	**SS**	**DF**	**MS**	**F (DFn, DFd)**	**P value**
Kv	0.4745	3	0.1582	F (1.000, 1.000) = 239.7	P=0.0411
Distance	5.921	11	0.5383	F (1.000, 1.000) = 17.15	P=0.1509
Kv x Distance	0.1743	33	0.005281	F (1.000, 1.000) = 1.801	P=0.4077
Subject x Kv	0.001979	3	0.0006597		
Subject x Distance	0.3453	11	0.03139		
Subject	0.2109	1	0.2109		
Residual	0.09677	33	0.002932		
Data summary					
Number of columns (Distance)	12				
Number of rows (Kv)	4				
Number of subjects (Subject)	2				
Number of missing values	0				

Table 10: Statistical analysis for 2 vs 3 implants for medium field of view with varying kVp

Table Analyzed	3 impl 90KV 5x5 vs 10x5				
Two-way RM ANOVA	Matching: Both factors				
Assume sphericity?	No				
Alpha	0.05				
Source of Variation	**% of total variation**	**P value**	**P value summary**	**Significant?**	**Geisser-Greenhouse's epsilon**
mA	70.08	0.0345	*	Yes	0.1429
Distance	23.70	0.1585	ns	No	0.09091
mA x Distance	2.418	0.2753	ns	No	0.01299
Subject x mA	0.2061				
Subject x Distance	1.533				
Subject	1.550				
ANOVA table	**SS**	**DF**	**MS**	**F (DFn, DFd)**	**P value**
mA	32.79	7	4.684	F (1.000, 1.000) = 339.9	P=0.0345
Distance	11.09	11	1.008	F (1.000, 1.000) = 15.46	P=0.1585
mA x Distance	1.132	77	0.01470	F (1.000, 1.000) = 4.695	P=0.2753
Subject x mA	0.09646	7	0.01378		
Subject x Distance	0.7173	11	0.06521		
Subject	0.7252	1	0.7252		
Residual	0.2410	77	0.003130		
Data summary					
Number of columns (Distance)	12				
Number of rows (mA)	8				
Number of subjects (Subject)	2				
Number of missing values	0				

Table 11: Statistical analysis for comparison between small and medium fields of view for varying mA values (3implants)

Table Analyzed	5x5 vs 10x5 kV (Model 1 and 2) - 3implants				
Two-way ANOVA	Ordinary				
Alpha	0.05				
Source of Variation	**% of total variation**	**P value**	**P value summary**	**Significant?**	
Interaction	1.189	0.7942	ns	No	
kVp	9.295	<0.0001	****	Yes	
Distance	81.14	<0.0001	****	Yes	
ANOVA table	**SS**	**DF**	**MS**	**F (DFn, DFd)**	**P value**
Interaction	0.08198	15	0.005465	F (15, 72) = 0.6814	P=0.7942
kVp	0.6411	3	0.2137	F (3, 72) = 26.65	P<0.0001
Distance	5.597	5	1.119	F (5, 72) = 139.6	P<0.0001
Residual	0.5775	72	0.008021		
Data summary					
Number of columns (Distance)	6				
Number of rows (kVp)	4				
Number of values	96				

Table 12: Statistical analysis for comparison between small and medium fields of view for varying kVp values (3implants)